AD-A057 804 IOWA STATE UNIV AMES ENGINEERING RESEARCH INST F/G 13/7
DEVIATION ANGLE / TURNING ANGLE PREDICTION FOR ADVANCED AXIAL-F--ETC(U)
DEC 77 G K SEROVY F33615-76-C-2090
UNCLASSIFIED ISU-ERI-AMES-78196 AFAPL-TR-77-81 NL

1 OF 2
AD A057804

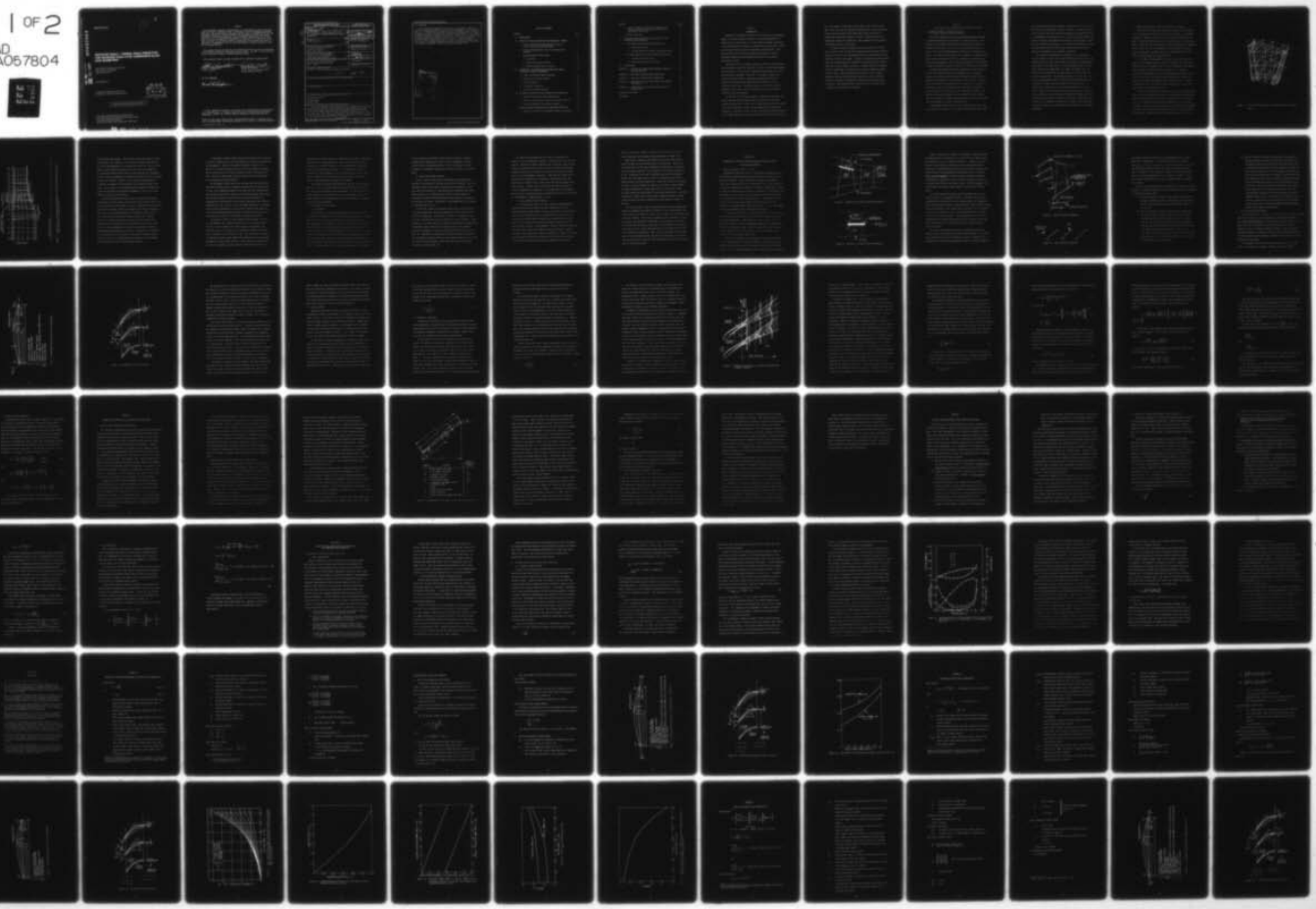

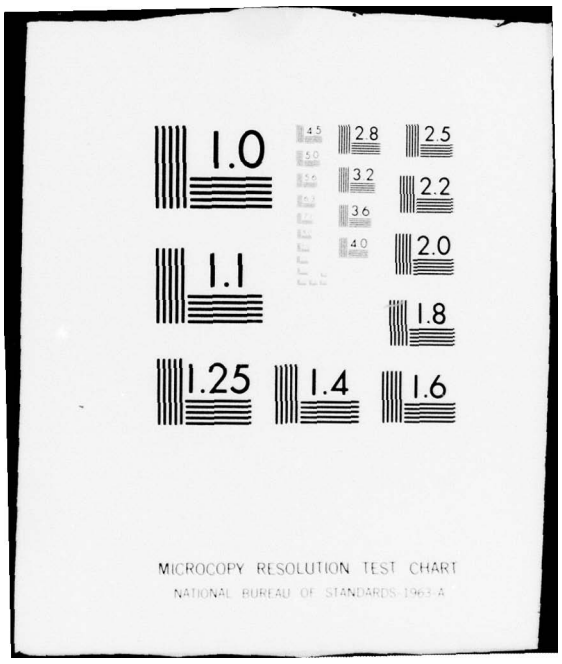
1.0
1.1
1.25
1.4
1.6
1.8
2.0
2.2
2.5
2.8
3.2
3.6
4.0
4.5
5.0
5.6
MICROCOPY RESOLUTION TEST CHART
NATIONAL BUREAU OF STANDARDS-1963-A

AFAPL-TR-77-81

DEVIATION ANGLE / TURNING ANGLE PREDICTION FOR ADVANCED AXIAL-FLOW COMPRESSOR BLADE ROW GEOMETRIES

ENGINEERING RESEARCH INSTITUTE
IOWA STATE UNIVERSITY
AMES, IOWA 50011

DECEMBER 1977

TECHNICAL REPORT AFAPL-TR-77-81
Final Report – April 1976 - November 1977

Approved for public release; distribution unlimited.

AIR FORCE AERO PROPULSION LABORATORY
AIR FORCE WRIGHT AERONAUTICAL LABORATORIES
AIR FORCE SYSTEMS COMMAND
WRIGHT-PATTERSON AIR FORCE BASE, OHIO 45433

NOTICE

When Government drawings, specifications, or other data are used for any purpose other than in connection with a definitely related Government procurement operation, the United States Government thereby incurs no responsibility nor any obligation whatsoever; and the fact that the government may have formulated, furnished, or in any way supplied the said drawings, specifications, or other data, is not to be regarded by implication or otherwise as in any manner licensing the holder or any other person or corporation, or conveying any rights or permission to manufacture, use, or sell any patented invention that may in any way be related thereto.

This report has been reviewed by the Information Office (OI) and is releasable to the National Technical Information Service (NTIS). At NTIS, it will be available to the general public, including foreign nations.

This technical report has been reviewed and is approved for publication.

Arthur J. Wennerstrom
ARTHUR J. WENNERSTROM
Project Engineer

Walker H. Mitchell
WALKER H. MITCHELL
Acting Chief, Technology Branch
Turbine Engine Division

FOR THE COMMANDER

Ernest C. Simpson

"If your address has changed, if you wish to be removed from our mailing list, or if the addressee is no longer employed by your organization please notify AFAPL/TBC *,W-PAFB, OH 45433 to help us maintain a current mailing list".*

Copies of this report should not be returned unless return is required by security considerations, contractual obligations, or notice on a specific document.

AIR FORCE/56780/11 July 1978 — 200

SECURITY CLASSIFICATION OF THIS PAGE *(When Data Entered)*

REPORT DOCUMENTATION PAGE

READ INSTRUCTIONS BEFORE COMPLETING FORM

1. REPORT NUMBER: AFAPL-TR-77-81	2. GOVT ACCESSION NO.
3. RECIPIENT'S CATALOG NUMBER	
4. TITLE *(and Subtitle)*: DEVIATION ANGLE / TURNING ANGLE PREDICTION FOR ADVANCED AXIAL-FLOW COMPRESSOR BLADE ROW GEOMETRIES	5. TYPE OF REPORT & PERIOD COVERED: Final Report, 1 April 1976 – 30 November 1977,
	6. PERFORMING ORG. REPORT NUMBER: ISU-ERI-Ames-78196, TCRL-8
7. AUTHOR(s): George K. Serovy	8. CONTRACT OR GRANT NUMBER(s): F33615-76-C-2090
9. PERFORMING ORGANIZATION NAME AND ADDRESS: Engineering Research Institute, Iowa State University, Ames, Iowa 50011	10. PROGRAM ELEMENT, PROJECT, TASK AREA & WORK UNIT NUMBERS: Element: 61102F; Proj: 2307 Task: S1; Work Unit: 33
11. CONTROLLING OFFICE NAME AND ADDRESS: USAF Air Force Systems Command Hq., 4950th Test Wing, 4950/PM ES, Wright-Patterson AFB, Ohio 45433	12. REPORT DATE: December 1977 13. NUMBER OF PAGES: 116
14. MONITORING AGENCY NAME & ADDRESS *(if different from Controlling Office)*: Air Force Aero Propulsion Lab./TBX, Wright-Patterson Air Force Base, Ohio 45433	15. SECURITY CLASS. *(of this report)*: Unclassified 15a. DECLASSIFICATION/DOWNGRADING SCHEDULE

16. DISTRIBUTION STATEMENT *(of this Report)*

Approved for Public Release; distribution unlimited.

16 2307 12 S1

17. DISTRIBUTION STATEMENT *(of the abstract entered in Block 20, if different from Report)*

18. SUPPLEMENTARY NOTES

19. KEY WORDS *(Continue on reverse side if necessary and identify by block number)*

axial-flow compressor
cascade flow
deviation angle
turning angle

20. ABSTRACT *(Continue on reverse side if necessary and identify by block number)*

Axial-flow compressor design systems utilize experimentally-supported methods for estimation of fluid turning angles in individual blade rows. The three principal prediction methods now in use were developed during the period 1945 to 1960. There has been no substantial modernization of these procedures since 1960, while the methods have been widely applied to airfoil section profiles and in aerodynamic regions far outside the limits suggested by the original derivations and data correlations.

(continued) → next page

DD FORM 1 JAN 73 1473 EDITION OF 1 NOV 65 IS OBSOLETE

404 418

SECURITY CLASSIFICATION OF THIS PAGE *(When Data Entered)*

20. Continued.

This investigation indicates that there is not enough new linear and compressor cascade experimental data to support development of a new correlation. It is suggested that a modification of the deviation angle correlation originally proposed by the National Gas Turbine Establishment (U. K.) should be attempted, and that the modified correlation should correct for the effects of several aerodynamic variables interacting in the viscous flow region on the suction surfaces of the cascade airfoil profiles. A term including the diffusion loading parameter D_{eq} might be added to the NGTE correlation equation because of the known relationship between this parameter and the growth and separation tendencies of the suction surface boundary layer.

sub eq

TABLE OF CONTENTS

SECTION I

INTRODUCTION

Design point performance levels for axial-flow fan and compressor stages in aircraft propulsion systems have increased significantly during the past several years. To reach these performance objectives it has been necessary to control the flow field in the entrance, internal flow path and exit regions of compressor configurations. This design control calls for the continuous development of realistic aerodynamic models and corresponding solutions of the equations describing the flow.

In the past, and at present, compressor flow field solutions have used substantial input from experimental research in which measurements have been made in actual fan and compressor flow passages or in flows simulating real compressor conditions. For example, almost total reliance has been placed on experimentally-supported methods for prediction of fluid turning angles and total-pressure losses in individual blade rows. Compressor design is, as a result, heavily dependent on the quality of the experiments and data correlations associated with these methods.

In the case of flow turning angles in compressor blade rows, the three principal currently-used prediction methods were developed during the period 1945 to 1960. One of these methods directly predicts fluid turning angles in terms of cascade geometry and aerodynamic parameters. The others predict the exit flow deviation angle, defined as the angle between the average exit flow direction and the direction

of a line tangent to the blade section camber line at the trailing edge. There has been no substantial modernization of these deviation/turning angle procedures since 1960, while during this time the methods have been widely applied to airfoil section profiles and in aerodynamic regimes far outside the limits suggested by the original derivations and data correlations.

The present study was initiated with three objectives in mind. First, recent trends in axial-flow compressor design systems should be examined in order to set reasonable qualitative requirements for estimation of relative flow angles. Second, the existing deviation/turning angle correlations should be reexamined to define the areas in which they fail and the reasons for failure. Finally, specific recommendations for improvement in deviation/turning angle prediction methods should be made. These methods should be useful for the ranges of geometric and flow field parameters expected to occur in advanced axial-flow compressor configurations during the foreseeable future. Furthermore, they should produce results which are compatible with contemporary design system flow models.

SECTION II

AXIAL-FLOW FAN AND COMPRESSOR DESIGN/ANALYSIS SYSTEMS

1. CURRENT FLOW MODEL--STEADY RELATIVE FLOW OF A LOCALLY INVISCID CONTINUOUS MEDIUM

Flow field computation in axial-flow compressors must be based on aerodynamic models much less complex than the real flow. It is necessary in evaluation and application of possible flow models to consider not only what realistically can be computed but also the nature of the flow field measurements available for verification of results. The intent in this section is to describe a compressor flow model useful in the main stream of an aerodynamic design system for research and development, and to discuss the qualitative requirements of such a flow model in terms of estimation of blade row flow turning.

Contemporary design and analysis computation of axial-flow compressor flow fields is based on the assumption of a continuous medium, and on definition of the paths followed by fluid particles supposedly representing a valid average of the real flow. To determine these paths the flow relative to all blade rows is assumed to be steady, so that the average particle paths define streamlines, stream surfaces and stream tubes in the compressor flow path. The physical principles governing the flow include the laws of motion and of conservation of angular momentum and mass, as well as the laws and relationships of classical thermodynamics.

In applying these principles to the compressor flow field, the terms directly accounting for local shear stress effects have almost

always been omitted from the equations representing the laws of motion. The flow then is described as inviscid. However, the viscous effects in the flow are taken into account by entering the accumulated effects of thermodynamic irreversibility as an increase in entropy between the entrance condition and downstream locations in the flow field. While this is an artificial procedure, it is technically satisfactory except in regions where the local fluid shear stresses make an important numerical contribution in the equations of motion.

The conceptual development and refinement of the continuous, locally inviscid, steady relative flow model has occurred over a considerable period of time, and includes, for example, contributions by Lorenz (Ref. 1), Traupel (Ref.2), Wu and Wolfenstein (Ref. 3 and 4), Hatch, Giamati and Jackson (Ref. 5), Giamati and Finger (Ref. 6), Smith (Ref. 7), Novak (Ref. 8), Marsh (Ref. 9), Horlock (Ref. 10), Horlock and Marsh (Ref. 11), Wennerstrom (Ref. 12), Frost (Ref. 13), Stuart and Hetherington (Ref. 14), and Novak and Hearsey (Ref. 15). Examination of these references shows that the model itself, in general form, would permit a very detailed definition of the flow field. However, up to the present time, there have been no reported cases in which the flow field has been determined without additional assumptions concerning the character of the flow. Furthermore, the validity of the computed flow field is at present totally dependent on empirical input, a fact discussed in more depth in the following subsection.

2. CURRENT DESIGN/ANALYSIS FLOW FIELD COMPUTATION PROGRAMS

If the flow in an axial-flow compressor configuration is assumed to be continuous and steady relative to each blade row, it is possible to generate a schematic picture of the flow like that proposed by Wu (Ref. 4) using hub-to-tip (S_2) and blade-to-blade (S_1) stream surfaces. Figure 1 shows sets of these surfaces as they might appear if determined for one blade row. For an axisymmetric entrance region flow, these surfaces would have a periodic character, repeating exactly in each blade-to-blade passage in a given blade row.

It is evident from examination of Figure 1 that the flows on S_2 and S_1 stream surfaces interact, and that a change in the flow distribution on one set of surfaces will, in both a mathematical and physical sense, influence the flow field on the other set. It appears attractive and possible to set up the equations governing the flow on each set of surfaces, and to solve these equations in an iterative process to determine the shapes of the S_2 and S_1 surfaces. Specific computational trials of this nature have been made, but success has been limited at best (Refs. 14 and 15).

In current design/analysis systems for axial-flow compressors the flow field is predicted on both hub-to-tip and blade-to-blade surfaces. The interaction between these flows is recognized, but the surfaces are not true stream surfaces and only approximate S_2 and S_1 surfaces in shape. Fluid velocities and properties are computed on a designated hub-to-tip surface, and this information is used to locate the intersections with a radial-axial plane (meridional plane) of a set of

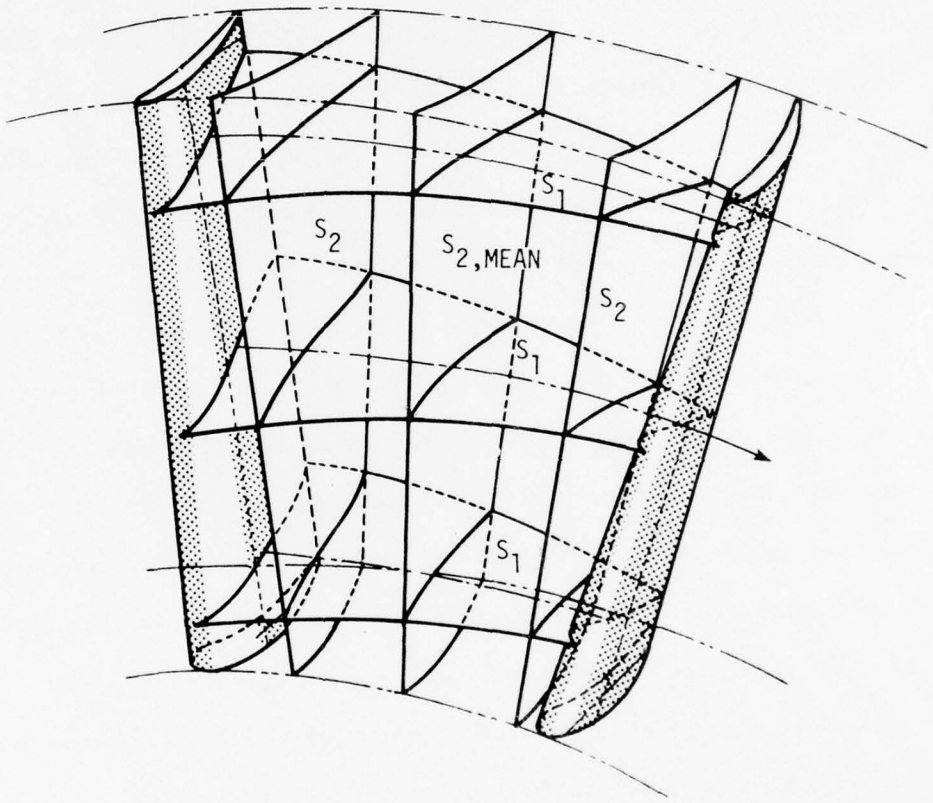

Figure 1. S_1 and S_2 Stream Surfaces in Blade-to-Blade Flow Passage [Ref. 4].

axisymmetric blade-to-blade surfaces of revolution. These surface are formed by rotation about the compressor axis of streamline approximations computed on the hub-to-tip solution surface.

A sample set of computed surface intersections is shown in Figure 2, replotted from Reference 16, in which the hub-to-tip solution was obtained by the method outlined in References 7 and 17. In design/analysis computation these intersections and the corresponding surfaces of revolution are thought of as control surfaces bounding specified fractions of the total compressor flow. They also locate the blade-to-blade surfaces for design/analysis, but the actual prediction of blade-to-blade flow patterns may not occur on the surfaces of revolution for reasons which are outlined later.

Hub-to-tip surface solutions for compressors usually assume that the continuous, steady relative flow is also locally inviscid and adiabatic. Determinations of the velocity and fluid property distributions are made at computing stations which are in reality control surfaces spanning the flow path from hub to tip. These control surfaces may be planes normal to the axis as in Figure 2 or they may be non-radial surfaces, possibly matched to the leading- or trailing-edge contour of a row of blades. Computing stations are in some design systems located only in the spaces between blade rows, and the hub-to-tip computation is then made on a radial-axial surface (meridional plane). Alternatively, there may also be computing stations located in regions within the blade rows. In this case the equations used in computing are related to the flow on a hub-to-tip surface located in

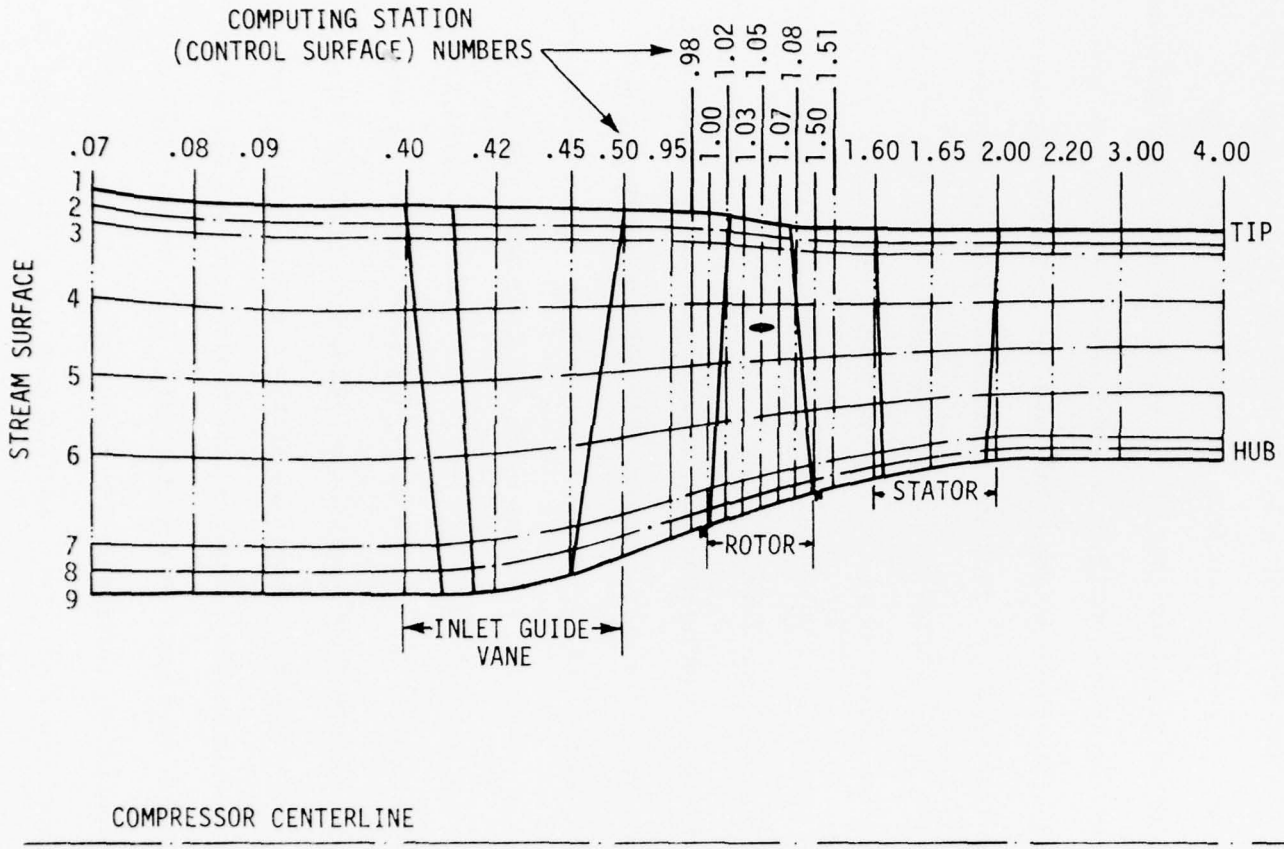

Figure 2. Intersection of Stream Surface Approximations with Meridional Plane Section of Axial-Flow Compressor Stage [Ref. 16].

the blade-to-blade channel. This surface is often described as a mean stream surface (see Figure 1), but in practical design computation it is only an approximation to a true mean stream surface. The real flow within a blade channel which turns the flow cannot be axisymmetric, but computations within blade rows are often described as axisymmetric because certain circumferential derivatives of velocity in the equations of motion are dropped. However, at the same time circumferential variations in pressure are accounted for by distributed "body" force terms. In any event, current design/analysis computation within compressor blade rows is not genuinely axisymmetric, and it is not performed on a mean S_2 stream surface.

No matter how the hub-to-tip solution is computed, it requires input which in effect defines the direction of the relative flow at the entrance and exit to each blade row, and for computation within the row the pattern of change in direction through the row must be estimated. There must also be some description of increases in entropy due to flow irreversibility across and through the blade row. However, relative flow angle and entropy increase can only be predicted for known flow paths through the blade row and these are the flow paths which are being approximated in the hub-to-tip solution procedure. Understanding this paradoxical situation is equivalent to recognition of the interaction of the S_2 and S_1 stream surface flows mentioned earlier as well as to understanding of the importance of mechanisms for predicting the flow on blade-to-blade surfaces.

In contemporary design systems, blade-to-blade flow field solutions are usually computed as an aid in optimizing the blade section shape and cascade geometry. However, the inputs found most critical to the quality of the blade-to-blade solution are the exit region flow angles and the stream tube area variation between the blade row entrance and exit. These are results that could only emerge from interactive hub-to-tip and blade-to-blade solutions.

The dependence of both hub-to-tip and blade-to-blade solutions on input which includes direct or indirect specification of the direction of flow at the computing stations is the basis for this investigation. Until workable interactive compressor flow field solutions appear which directly and internally account for the real fluid influences of compressibility and viscosity on flow angles and losses, some external mechanism will have to exist to allow for these influences. At present these external mechanisms are in the form of relative flow angle and low estimation methods primarily based on analysis and correlation of experimental data from real or simulated compressor blade rows.

To summarize, typical current design/analysis programs are based on the assumption of a steady relative flow of a continuous medium. The flow is also assumed to be locally inviscid and adiabatic, but cumulative effects of viscosity are included by allowing the entropy level to change in the direction of flow. The flow field is estimated by computation using a single hub-to-tip solution surface and multiple axisymmetric blade-to-blade surfaces. These surfaces are intersected by arbitrary computing stations (control surfaces) where the fluid

properties and velocity vectors are numerically determined. The hub-to-tip surface is an approximation to a mean stream surface, and it is assumed to be a surface on which correct blade-to-blade averages of velocity and fluid properties exist. The axisymmetric surfaces of revolution are approximations to blade-to-blade stream surfaces, and they are assumed to be surfaces which can be used to trace fluid particle paths through the compressor flow passage.

Some example aerodynamic design/analysis systems are described in Refs. 17 to 25. All of the hub-to-tip solution procedures fall into the class called streamline curvature methods. All of the systems include mechanisms for estimation of relative flow angles and thermodynamic losses, and the mechanisms are basically prediction equations derived from experimentation.

3. DESIGN/ANALYSIS SYSTEM TRENDS

a. Flow Model

The potential for a major breakthrough in the basic flow model must always be considered, and the most obvious opportunity for development in this area is in the computation of unsteady flow effects including blade row interaction. In order to do this the coordination between hub-to-tip and blade-to-blade solutions would have to be improved, and there is a strong possibility that the concept of streamline curvature solutions for sets of S_2 and S_1 surface approximations would have to be discarded. There have been some reported computation procedures which could be developed in the direction of a very general flow model, for example Reference 26, but the current state of this work is

such that much more exploratory effort will be required. However, considering the substantial evidence that the assumption of steady relative flow is questionable (Refs. 27-29), the influence of this assumption on aerodynamic design quality should continue to be investigated.

b. Hub-to-Tip Surface Solution

Recent trends in design system development have emphasized improvement in the quality of the hub-to-tip surface solution. There are additional areas in which these solutions may be developed, but the most important potential for improving solution agreement with experimental evidence is in finding better and more reliable means for obtaining the blade-to-blade performance used as input to the hub-to-tip solution iterations. Discussion of this possibility is the subject of the subsection (II.3.c).

The end wall regions in compressor blade rows, near the hub and tip passage boundaries, have been inadequately handled in hub-to-tip flow field computation. The problem is in part a consequence of the fact that the hub-to-tip flow is assumed to be locally inviscid. These regions were initially taken into account by introduction of empirically established annulus effective area blockage factors with possible additional adjustments to energy transfer within the end wall region (Ref. 6). Subsequent accounting has included replacement of empirical area blockage by computed effective area blockage (Refs. 24, 30, 31) and more detailed analyses (Refs. 32,33) which have not given entirely satisfactory results (Ref. 34).

The complex three-dimensional wall flows in compressors are evidence of the non-negligible influence of shear stress terms in those regions. Additional progress should be made in the near future by providing new experimental and analytical input to hub-to-tip solutions. Consideration must also be given to limits on the validity of axisymmetric or quasi-axisymmetric solutions. Some time ago, Smith (Ref. 7) showed that the assumption of axisymmetric flow becomes weaker for high blade row loading levels. This conclusion has been supported by other analyses. However, until the present time there has been no criterion suggested for prediction of a loading limit for axisymmetry, while practical considerations have allowed few real trials in the field of nonaxisymmetric computing (Refs. 15, 35).

c. Blade-to-Blade Surface Solution

It has already been noted that most compressor design/analysis systems include blade-to-blade flow field computation to aid in optimizing blade section shapes and their orientation in the blade row, but it must be remembered that the optimization is carried out in an iterative procedure in which the hub-to-tip distribution of flow is used to set the upstream and downstream boundary conditions for the blade-to-blade solution. These boundary conditions include the upstream and downstream relative flow angles and stream tube areas. However, even under these conditions a complete capability to compute the viscous and compressible blade-to-blade surface flow field in axial-flow compressor blade row geometries has not been demonstrated up to the

present, because this complete capability would include satisfactory direct prediction of flow angles and losses within the blade rows.

Many partial computation procedures do exist for blade-to-blade flows and these are the procedures used in optimization. Nearly all, for example Refs. 36-40, begin computation by working with an inviscid flow, and viscous influences are introduced in an iterative sequence if at all. References 36, 41 and 42 represent some specific attempts to predict exit flow angles and/or losses for compressor blade rows by blade-to-blade flow field computation. These were constructive attempts but there is little evidence of regular use of these or other methods to replace experimental turning angle and loss correlations in the iterative hub-to-tip calculations of an overall design system. Increased utilization of high relative Mach numbers combined with high loading levels has made the task of prediction even more difficult (Refs. 43 and 44).

The current overall trend in blade-to-blade flow field computation appears to emphasize development of ability to control and optimize the flow patterns in the blade row rather than to predict the flow deflections and losses produced. Under these circumstances the continuation of both qualitative and quantitative improvement of experimental correlations for turning angle and loss is essential, but the possibility of improvement exists only if a basic conceptual model of the blade-to-blade flow is established and understood. There are now differences in the models used in various design systems, and one of the functions of the following two sections is to describe these differences and fix on a preferred base for the present study.

SECTION III

TERMINOLOGY, DEFINITIONS AND EQUATIONS FOR AIRFOIL SECTIONS IN CASCADE ARRANGEMENT

1. LINEAR AND ANNULAR AIRFOIL CASCADES

Substantial differences exist in conventions and methods used in description of compressor blade row geometry and in reporting of aerodynamic performance. These differences contribute to problems encountered in comparison of sets of experimental data and in comparison of compressor geometries originating in different organizations. While it might be constructive to establish a standard set of definitions and procedures, it is not likely that a consistent and acceptable scheme can be defined for all users and applications. The function of this section is to set up a basic system for this report and to call attention to situations where questions may occur. It may also suggest that some uniformity could be developed in the future.

The remainder of the report concerns estimation of the quantitative flow turning characteristics of rows of blade as actually utilized in axial-flow compressors. Discussion here, first relates to the row geometries found in research, development and production compressors, but must also consider linear or plane row geometries used to experimentally simulate some of the features of flow in compressor rows. Figures 3a and 3b represent these cases.

Section II discussed flow on axisymmetric blade-to-blade stream surface approximations and through axisymmetric stream tube approximations which intersect axial-flow compressor blade rows and thereby define a series of blade section profiles in annular cascade arrangement.

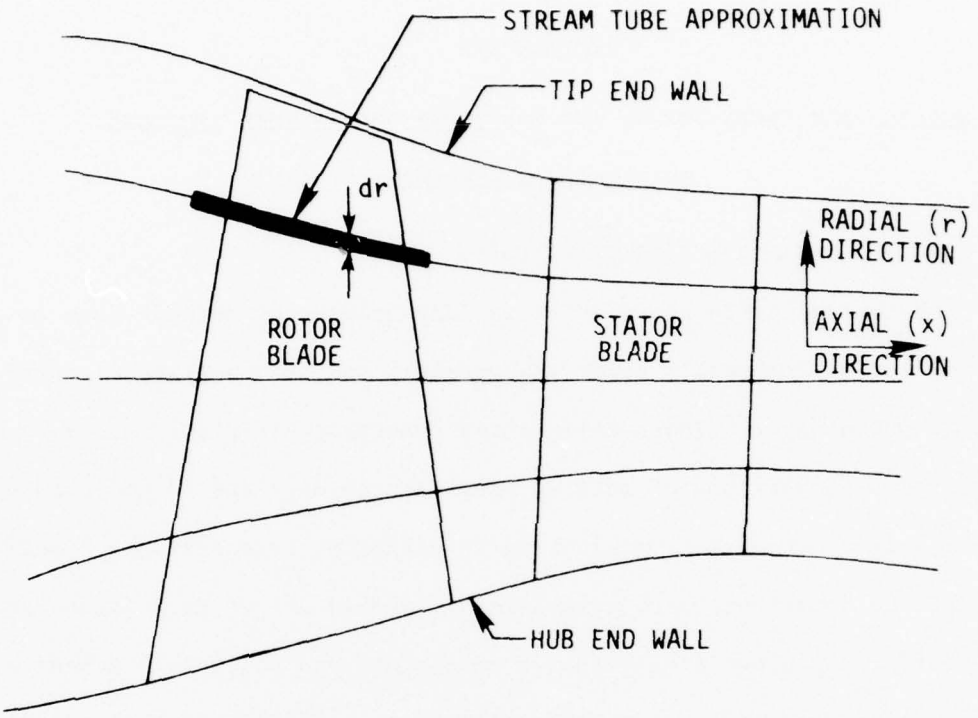

Figure 3a. Definition of Annular Cascade Arrangement.

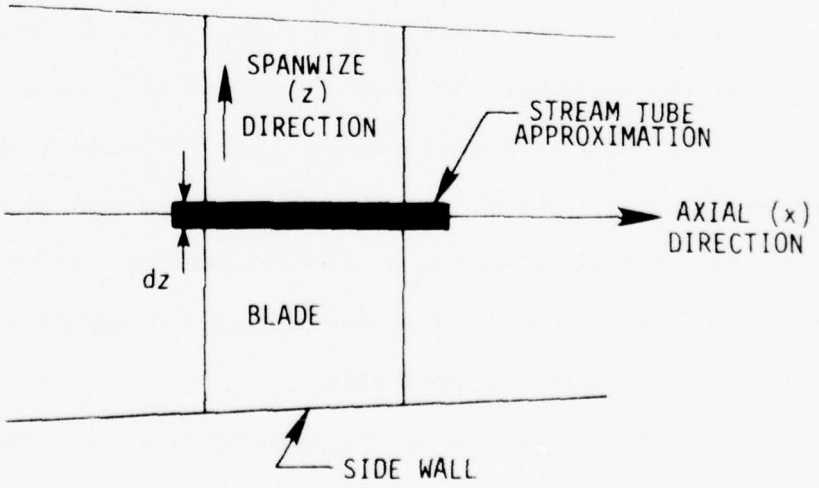

Figure 3b. Definition of Linear Cascade Arrangement.

Linear or plane rows of blades in a rectangular channel represent a conventional but controversial way to study flow in a geometry somewhat similar to that of a compressor blade row. A model of the flow through a linear blade row could also involve interacting sets of stream surface approximations with nearly plane blade-to-blade stream surface/stream tube approximations intersecting the row to define a plane cascade arrangement. Annular and plane cascade arrangements corresponding to Figures 3a and 3b are shown in Figures 4a and 4b as they appear when laid out on a plane surface. The term cascade is used in this report to describe either annular or plane airfoil section arrays.

In a plane cascade the blades almost invariably have the same section profile at all spanwise locations. The plane stream surface approximation is satisfactory for the mid-span region of contemporary linear cascade test facilities. This means that a blade-to-blade stream tube near the center of the cascade span as in Figure 3b has the same z location at all values of x and y, and that thickness dz is constant from blade to blade at a given x. The thickness dz may vary with x, depending on the cascade facility aspect ratio, the shape of the side walls and the removal or recirculation of flow through slotted or porous side walls.

In nearly all compressor blade rows the individual blades are twisted and have different section shapes along the span. This continuous variation in section and variation in radial coordinate of the axisymmetric stream surface approximations with x as shown in Figure 3a

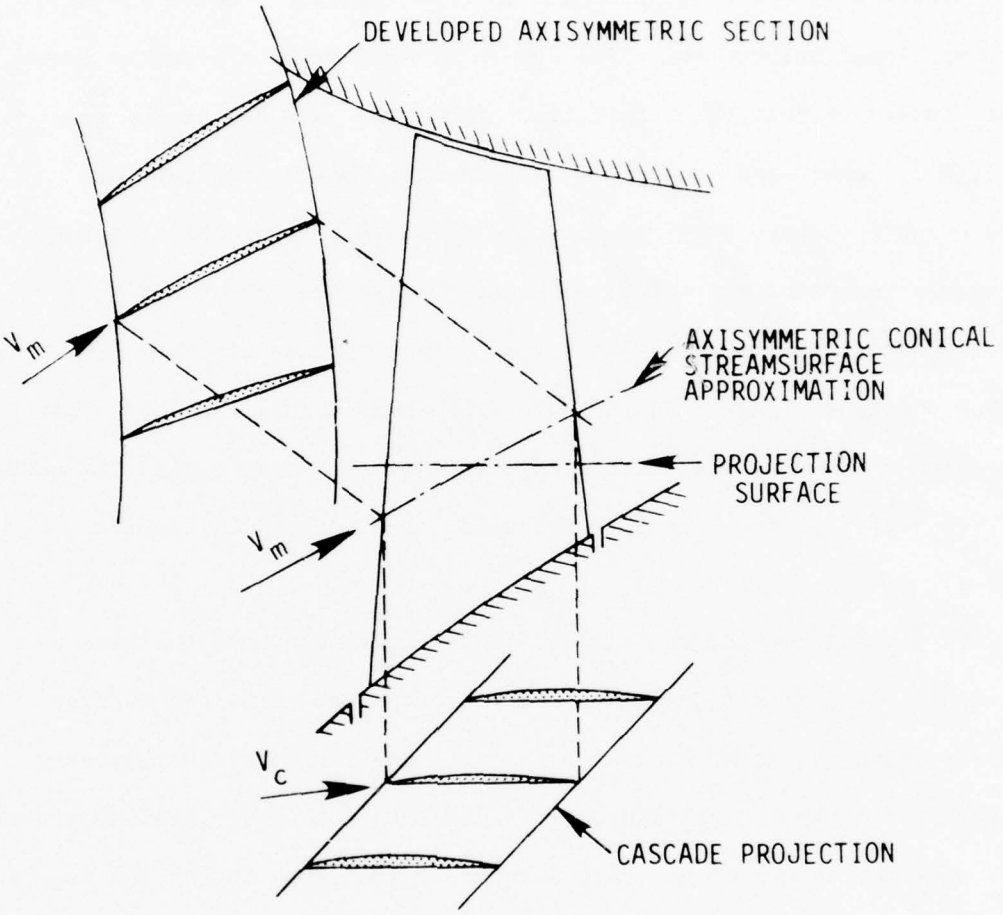

Figure 4a. Annular Cascade Arrangements.

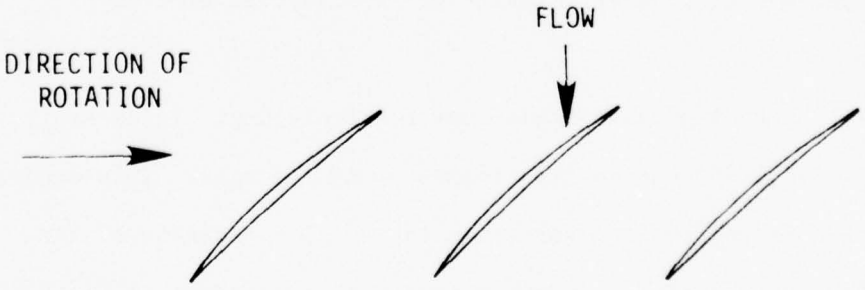

Figure 4b. Linear Cascade Arrangement.

are primary reasons for difficulty in describing effective cascade geometries in compressors. It should be noted that in a fashion analogous to the linear cascade, the axisymmetric stream surface/stream tube approximation means not only that each stream surface has the same r coordinate for all θ values at a given x, but that each stream tube has the same thickness dr for all θ values at a given x. Each stream tube approximation may have both variable radius and thickness as x changes.

There are three common methods for definition of effective cascade geometry for compressor design and analysis purposes when the axisymmetric stream surface model is used:

(a) The flow follows the computed stream surface approximation through each blade row and is influenced by the exact blade surface shape intersected by the stream surface (Refs. 24, 45, 46, 47).

(b) The flow follows the computed stream surface approximation through each blade row but is influenced by an effective cascade defined by the intersection of a conical surface with the row. This surface passes through the leading and trailing edges of each blade at the same radial locations as the computed stream surface (Ref. 48). This simplifies the layout process for the cascade because the conical intersection surface can be readily developed on a plane. Figure 4a shows this type of development.

(c) The flow follows the computed stream surface approximation through each blade row but is influenced by an effective cascade geometry which is determined by projecting radially onto a cylinder the stream surface intersection with the blade row. This effective cascade is called the spanwise cascade projection and in situations where the change in stream surface radius is significant the effective cascade is substantially different from those which would result from procedures such as (a) and (b). The fluid velocities influenced by the cascade plane projection are the resultant of the local axial and circumferential components and therefore neglect the radial component (Refs 17, 49). The radius of the cylinder for projection is usually taken as the average of the corresponding stream surface radii at blade row leading and trailing edges. Figure 4a also shows this development.

2. BLADE SECTION PROFILE GEOMETRY

In linear and annular cascades, the stream surface approximation intersection and the effective cascade geometry concept applied combine to give a blade section profile for the individual airfoils expected to influence the flow. Obviously the blade section profile must have a significant effect on cascade aerodynamic behavior. One of the major continuing problems in compressor design has been the determination of the most important profile geometric variables from the point of view of performance optimization.

For compressor blade section profile description as for all airfoils, it is necessary to define a reference line and an initial

coordinate point on that line. The recommended line in this study is the section chord line. The base point for profile construction is at X = 0, Y = 0 as shown on Figure 5. The base point (0,0) is the initial point on the section camber line, which is the skeleton of the blade section and describes its basic curvature. The camber line begins and ends on the chord line and the distance between the initial and final points is the section chord length c. The X, Y coordinates of the camber line are given as fractions of chord length. The camber line shape can be partially described by the position of the maximum camber point a and the maximum camber b. These variables are shown in Figure 5 for a blade section camber line with continuous positive camber. For many camber line shapes lines drawn tangent to the camber line at the initial (leading) and final (trailing) points are used as reference lines for flow angle measurement. These lines intersect to define a blade section camber angle φ as shown on Figure 6. It must be possible to construct camber lines with camber angles ranging from negative values to large positive values for a given value of a/c. Several methods exist for doing this and they are discussed in references associated with Section IV and Appendices A, B, C and D.[1]

[1] Camber line shapes may be generated which have a negative camber segment and an inflection point. In these cases the leading and trailing point tangent lines are used as reference lines for flow angle measurement but an effective camber angle is recommended for use in turning angle prediction in this report. See Section IV.2. Some camber lines such as the NACA a = 1.0 shape have leading and trailing point tangent line slopes giving an indeterminate or erroneous camber angle. In these cases an equivalent camber line may be used to define camber line slopes and an equivalent camber angle. See Appendix B for an example of this approach.

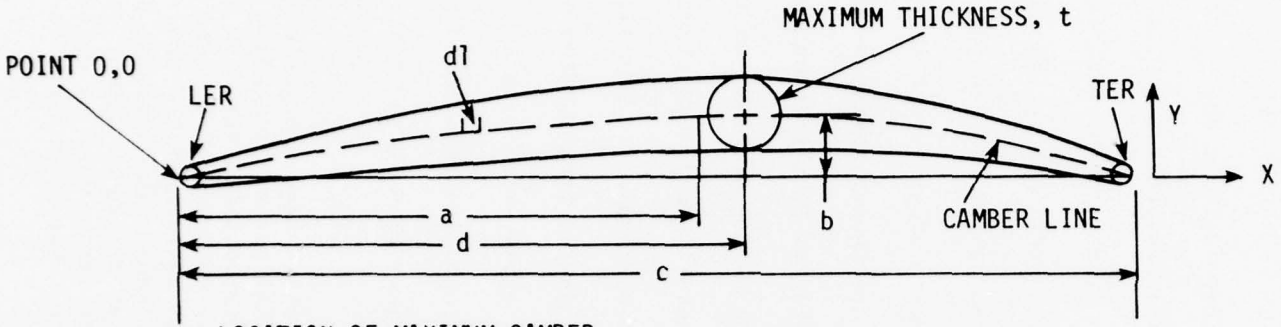

a = LOCATION OF MAXIMUM CAMBER

b = COORDINATE OF MAXIMUM CAMBER

c = CHORD LENGTH

d = LOCATION OF MAXIMUM THICKNESS

l = LENGTH OF CAMBER LINE MEASURED ALONG CAMBER LINE ARC

LER = LEADING EDGE RADIUS

TER = TRAILING EDGE RADIUS

Fig. 5. Recommended Blade Section Profile Terminology

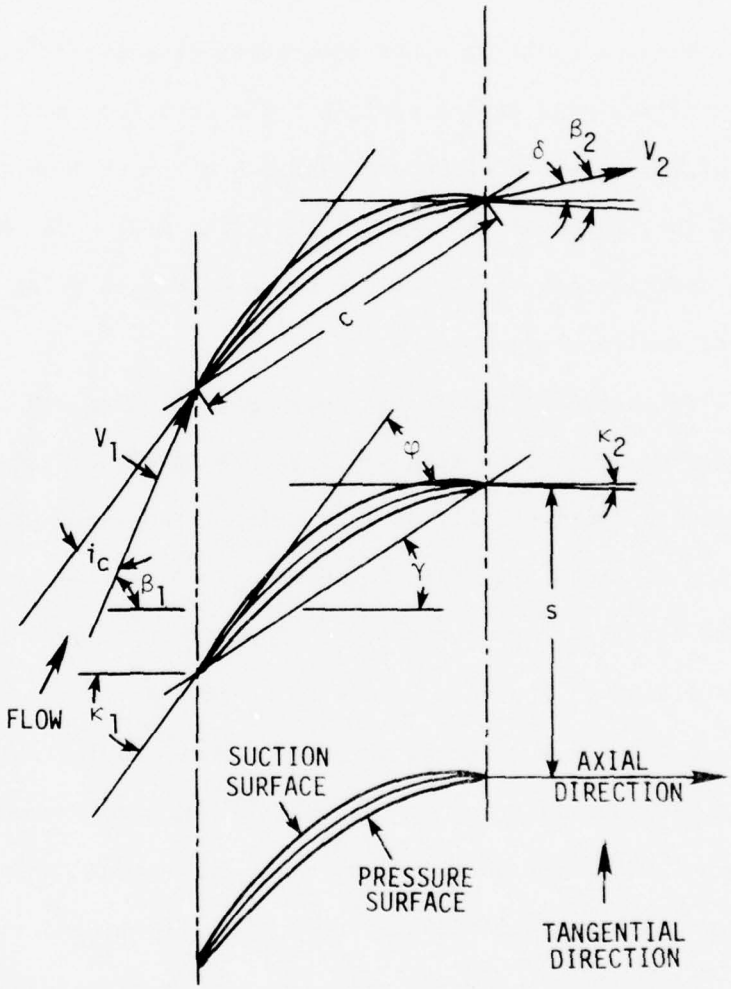

Figure 6. Recommended Cascade Terminology.

The construction of a typical blade section profile is completed by the addition of a profile thickness distribution to the camber line shape. The thickness distribution characteristics most frequently used in profile classification are the maximum thickness, the location of maximum thickness, and the radii or other describing dimensions for the leading edge and trailing edge of the profile. The location and value of maximum thickness may be given as fractions of chord line length (t/c, d/c) or of the length of the camber line (t/l, d/l). The standard thickness distribution variables are shown on Figure 5 for circular-arc leading-and trailing-edge shapes.

Until recent years almost all compressor blading was based on a few related sets of airfoil section profiles. A specific blade section profile combined an analytically defined camber line shape with a standard distribution of section profile thickness, supplemented by designated leading and trailing edge geometries. Some frequently-mentioned combinations are listed in Appendix D with references given for construction and layout details. Additional details on some combinations may be found in Appendices A, B and C. Not all of the combinations of Appendix D have been extensively used in compressor design, and only a few have been systematically evaluated to determine aerodynamic performance, either in compressor (annular cascade) or linear cascade arrangements.

Development of advanced fan and compressors has shown that improved performance can be obtained by design techniques which use arbitrary camber line shapes to optimize the blade-to-blade flow field. These camber lines do not have an established analytical shape, and may

exhibit camber line angle variations and maximum camber locations outside the conventional regimes used in the past. As a result, attention was focused in this investigation on the special problem of selecting or redefining geometric variables for classification and data correlation purposes when the blade section profiles are essentially arbitrary. These cases include the last two listed in Appendix D.

3. CASCADE GEOMETRY

Additional geometric variables are required to define a cascade arrangement of blade section profiles in a compressor blade row or in a linear cascade. In the linear cascade two variables are necessary and these are shown in Figure 6 as the blade chord angle or stagger angle γ and the blade tangential spacing s. The stagger angle is measured from the axial direction and the spacing is combined with the chord length to form the parameter solidity $\sigma \equiv c/s$. Figure 6 also shows κ_1 and κ_2, the cascade entrance and cascade exit camber line angles.

For the annular cascade arrangement in a compressor blade row the complexity of cascade geometry description increases considerably. There are problems in definition of both stagger angle or camber line angle and solidity. As shown in Figure 3a the blade-to-blade stream surface approximation may have both variable radius and slope through the blade row. The definitions of camber line or chord line direction and solidity then depend on the effective cascade geometry selection discussed in Section III.1. Some alternate procedures for camber line

and chord line are described in Refs. 47 and 48. The numerical value of solidity depends on both the chord length of the effective blade section and the radius used to determine the tangential spacing. The average of the leading-and trailing edge stream surface radii is frequently used so that

$$\sigma = \frac{c}{\frac{\pi(r_1 + r_2)}{N}} \tag{1}$$

4. AERODYNAMIC PARAMETERS

Following the selection of effective blade section profile and cascade geometries, and specifically the parameters needed to describe these geometries correctly for performance prediction, both independent and dependent aerodynamic variables must be defined. Again in this area there are questions and alternative possibilities.

In the region of the flow field immediately upstream from the cascade the significant independent variables are the fluid thermodynamic properties and the velocity magnitude and direction. These set the effective cascade fluid entrance angle on the stream surface approximation. This angle for a linear cascade is shown as β_1 on Figure 6. The inlet conditions also establish the entrance Mach number M_1, the flow field dynamic variable Reynolds Number Re, and the appropriate parameters describing the turbulence characteristics of the entrance flow. All of these parameters require careful definition because of the non-uniformity which exists in most entrance region fields.

References 44 and 50 give some options on averaging methods and on questions related to measuring correct values of entrance flow variables.

The entrance flow angle β_1 defines a subsidiary set of angles giving the inlet direction measured from a reference line fixed in the blade section profile geometry. The angles most frequently used in recent times have been the incidence angle measured from the camber line direction at the leading edge i_c and the incidence measured from a line tangent to the suction surface at the point where the leading edge shape fairs into the profile thickness distribution i_{ss}. However, the angle of attack α, referencing the entrance flow direction to the chord line direction in the cascade geometry, was the inlet flow parameter used in most systematic linear cascade experiments for reporting purposes (see Appendix B) and has been occasionally used in more recent experimental work. Figure 6 shows the incidence angle referenced to the camber line direction.

In both linear and annular cascade arrangements geometric and aerodynamics conditions set a final independent variable which represents a streamtube area ratio. The variable is commonly fixed by setting the ratio of the axial velocity-density products across the cascade. In this report the ratio is

$$\Omega \equiv \frac{\rho_2 V_{x,2}}{\rho_1 V_{x,1}} \tag{2}$$

The variable Ω has an important influence on both subsonic and supersonic cascade flows and its components must be determined on a rational and comparable basis for use in compressor design. The averaging of data at cascade entrance and exit for computation of axial velocity and density (Ref. 50) should be done in a consistent manner as is discussed in connection with the evaluation of independent cascade performance parameters in the following paragraphs.

A schematic representation of the velocity distribution at the exit of a cascade of blade section profiles is shown in Figure 7. Although this Figure shows only a possible distribution of velocity, the real flow field involves variations with the tangential or circumferential coordinate of total and static pressure, and of flow angle. For compressor cascade arrangements, the total temperature will vary as well, although in linear cascade experiment the total temperature is generally constant in the flow field. From the variable property and angle values, velocity averages must be found which are used in the determination of exit flow field parameters. These parameters are required to be satisfactory for the input to a design system computation for the hub-to-tip flow on a specified surface, and this means that the averages specified must have a real physical significance in representing an effective entrance condition for downstream blade rows.

Analysis of existing sets of experimental data for linear cascades and stationary annular cascades is difficult because, except for very recent data, the locations of measuring stations, characteristics of instrumentation and details of data reduction are insufficient to allow

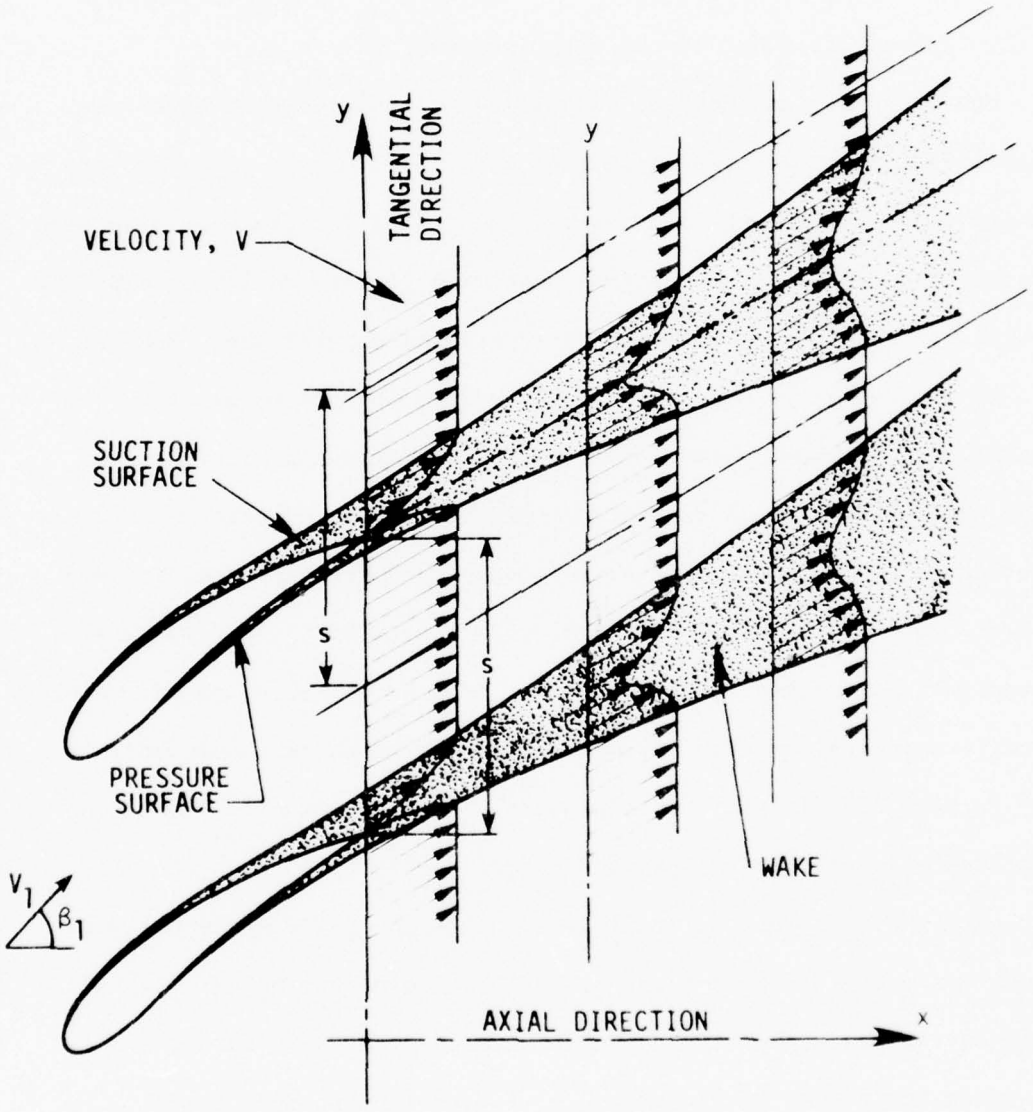

Figure 7. Schematic Representation of Velocity Distributions in Wake of Cascade.

conversion to a standard basis. In the case of measurement at the exit of rotating cascades these factors are compounded by a lack of understanding of the averaging behavior of stationary instruments exposed to the unsteady flow due to the rotating row.

Equations for computation of several possible cascade blade-to-blade averages of measured conditions are given in Ref. 50, with more details available in Ref. 51. Many sets of data for cascades have been reduced by a simple area-averaging method applied to variable values in the flow at cascade entrance and exit measurement stations. The use of mass-flow-weighted average variable values appears to be more reasonable. However, averaging all measured variables by either of these methods leads to inconsistent computed values of velocity and performance variables. This feature of data reduction was noted in 1956 in Refs. 52, 53 and 54. The idea of what are currently called two-dimensional momentum values, consistent mean values or mixed-out values of performance-determining variables was developed for incompressible flow in Refs. 52-54, and for compressible flow in Ref. 55. A similar data reduction method was derived in Ref. 56, in Ref. 57 as the consistent mean value method, and in Ref. 51 as the two-dimensional momentum method. Similar techniques are used in Refs. 58 and 59 to obtained mixed-out values. All of these procedures are based on the idea of computing the values of flow field variables (for example, total pressure) that would be realized if a non-uniform blade-to-blade distribution of the variables could be converted to a uniform set of the same variables in an adiabatic process obeying the conservation laws for

tangential and axial momentum as well as mass. When the terms fully-mixed or mixed-out are used there might be some confusion about the mixing process, but it is certain that the basic concept underlying the methods of Refs. 50-59 is the same.

The dependent performance variables determined from any selected averaging method are the cascade exit flow velocity, total pressure and static pressure. Each of these average values depends on the location of the exit reference plane, but for design/analysis purposes the location of the prediction station of most significance is at the line connecting the cascade blade section trailing edges. The usual performance parameters computed from the average values and used for prediction are the deviation angle, defined as the angle between the average flow direction at the trailing edge location and the camber line direction at the trailing edge, and a total-pressure loss coefficient, defined as

$$\bar{\omega} = \frac{\bar{P}_{2,\,ideal} - \bar{P}_2}{\bar{P}_1 - \bar{P}_1} \tag{3}$$

The deviation δ is shown for the linear cascade case in Figure 6 and for the annular cascade is referenced to the camber line direction on the axisymmetric stream surface approximation. For the linear cascade and for non-rotating annular cascades

$$\bar{P}_{2,\,ideal} = \bar{P}_1$$

but for the rotating annular cascade the definition uses total pressures measured relative to the rotating blade row so that

$$\bar{\omega}_{rel} = \frac{\bar{P}_{2,\ ideal\ rel} - \bar{P}_{2\ rel}}{\bar{P}_{1,rel} - P_1} \tag{4}$$

with (Ref. 60)

$$\bar{P}_{2,\ ideal\ rel} = \bar{P}_{1,\ rel} \left\{ 1 + \frac{\gamma - 1}{2} M_R^2 \left[1 - \left(\frac{r_1}{r_2} \right)^2 \right] \right\}^{\frac{\gamma}{\gamma - 1}} \tag{5}$$

$$M_R = \frac{U_2^{\,2}}{a_{o,1}^{\,2}}$$

Some alternative and additional cascade dependent variables for describing the cascade exit flow direction have been used or proposed. The greater part of the systematic linear cascade data was originally correlated in terms of flow turning angle (for examples, see Appendices B and C), and various parameters including the cascade blade section circulation

$$\Gamma = \frac{2\pi\ (r_1\ V_{\theta,1} - r_2\ V_{\theta,2})}{N} \tag{6}$$

have been suggested for correlation of turning.

In subsequent sections of this report, the quantitative characteristics of blade section profile boundary layers will be considered as they relate to both flow angle and total-pressure loss correlation. The

primary parameters of interest include the displacement (δ^*) and momentum (θ^*) thicknesses of the blade suction and pressure surface boundary layers, and the form factor relating these thicknesses. The thicknesses are fully defined in Refs. 55, 52 and 53. Ref. 52 and 61 show that for incompressible, two-dimensional cascade flow the boundary layer parameters are related to the total pressure loss coefficient by the equation

$$\bar{\omega}_p = 2\left(\frac{\theta^*}{c}\right)_2 \frac{\sigma}{\cos\beta_2}\left(\frac{\cos\beta_1}{\cos\beta_2}\right)^2\left[1-\left(\frac{\theta^*}{c}\right)_2\frac{\sigma\, H_2}{\cos\beta_2}\right]^{-3}\left(\frac{2H_2}{3H_2-1}\right) \quad (7)$$

with $H_2 = \dfrac{\delta_2^*}{\theta_2^*}$

On the basis of the assumption that the terms including H_2 vary in only a limited range near 1.0 for typical cascade operation, the equation

$$\bar{\omega}_p = 2\left(\frac{\theta^*}{c}\right)_2 \frac{\sigma}{\cos\beta_2}\left(\frac{\cos\beta_1}{\cos\beta_2}\right)^2 \quad (8)$$

has been used to relate a loss parameter to the blade trailing edge total boundary layer momentum thickness

$$\frac{\bar{\omega}_p\cos\beta_2}{2\sigma}\left(\frac{\cos\beta_2}{\cos\beta_1}\right)^2 \approx \left(\frac{\theta^*}{c}\right)_2 \quad (9)$$

and further simplifying if $(\cos\beta_2/\cos\beta_1)^2$ is nearly 1.0

$$\frac{\bar{\omega}_p \cos\beta_2}{2\sigma} = \left(\frac{\theta^*}{c}\right)_2 \qquad (10)$$

The left-side terms in Equations (9) and (10) have both been used to correlate total-pressure loss measurements with the $\bar{\omega}_p$ understood to be the loss coefficient excluding cascade shock wave losses and of course mixing losses which occur in the exit region downstream from the cascade trailing edge. This portion of $\bar{\omega}_{total}$ has been described as a profile loss. Further discussion relating to this matter may be found in Refs. 17-25, 44 and 48.

For this report the components of the total $\left(\frac{\theta^*}{c}\right)_2$ due to the suction surface and pressure surface boundary layers are defined as

$$\left(\frac{\theta^*}{c}\right)_{2,ss}$$

and

$$\left(\frac{\theta^*}{c}\right)_{2,ps}$$

The boundary layer thicknesses δ^* and θ^* are those measured in the direction perpendicular to the blade section average outlet flow at the trailing edge.

The importance of the boundary layer parameters and their relationship to the trailing edge profile loss lies in the possibility of connecting the same boundary layer parameters to the deviation angle or cascade turning angle.

In addition to the profile losses encountered in cascade flows, which account for compressibility effects on the character of blade surface boundary layers, current design/analysis systems recognize two other sources of irreversibility (relative total pressure loss, entropy increase) in the blade-to-blade flow field. The first of these is the irreversibility or loss due to shock waves when relative entrance velocity is supersonic or when local supersonic velocities occur in the blade-to-blade passage. The second source of loss is the secondary loss which may be observed in a cascade section due to flows which are not modeled by the equations used to compute the flow field. Discussion of the details of both of these subjects is beyond the scope of this report. The presence of shock waves in the flow field and the effects of secondary flows do influence deviation/turning angle in compressor blade cascade arrangements. However, in this report this influence is considered to be principally one involving the effects of shock waves and secondary flows on the growth of blade surface boundary layers. To illustrate, the effect of a blade-to-blade shock wave on the characteristics of the boundary layer on a blade surface downstream of the interaction region has a direct influence on deviation/turning. However the effect on deviation/turning of the shock crossing the main stream in the channel is not large except as it affects the pressure distribution imposed on the boundary layer downstream from the shock. Deviation angle as well as profile loss are assumed to be dependent principally on the nature of the boundary layers on blade suction and pressure surfaces.

5. CASCADE DIFFUSION PARAMETERS

In subsequent sections cascade diffusion loading will be discussed as it relates to the numerical values of deviation/turning angles. Various parameters have been suggested as measures of diffusion for linear and annular cascade geometries (Ref. 60), but two have shown a high correlation with experience in terms of profile loss estimation. These are the parameters D (Ref. 60) and D_{eq} (Ref. 61), initially derived for two-dimensional linear cascade loss correlation, but later substantially extended and correlated to profile loss in the annular cascades of compressor blade rows. The equations in current use for definition of D and D_{eq} for annular cascade cases are

$$D = 1 - \frac{W_2}{W_1} \pm \frac{r_2 V_{\theta,2} - r_1 V_{\theta,1}}{(r_1 + r_2)\sigma W_1} \qquad \begin{matrix} + \text{ rotor} \\ - \text{ stator} \end{matrix} \tag{11}$$

and

$$D_{eq} = \frac{V_{m,1}\cos\beta_2}{V_{m,2}\cos\beta_1} \left[1.12 + 0.61 \frac{\cos^2\beta_1}{\sigma} K \right] \tag{12}$$

with

$$K = \tan\beta_1 - \frac{r_2}{r_1} \frac{V_{m,2}}{V_{m,1}} \tan\beta_2 - \frac{\omega r_1}{V_{m_1}} \left(1 - \frac{r_2^2}{r_1^2} \right)$$

The equations and the parameters were developed to measure diffusion loading at incidence angles near the minimum loss value for a given cascade geometry.

SECTION IV

SELECTION OF BASIS FOR FLUID TURNING ANGLE PREDICTION

1. BLADE-TO-BLADE STREAM TUBE APPROXIMATION

For compressor design purposes the locally inviscid, steady relative flow model and the concept of stream surfaces and stream tubes in the compressor flow path will continue to be used. There is also justification for approximation of blade-to-blade stream surfaces and stream tubes by axisymmetric surfaces and volumes of revolution. Schematic stream tube intersections with a meridional plane are shown in Figure 3a. The axisymmetric approximation means that while the radius r and the thickness dr may change in the x direction, r and dr do not change with θ at a fixed x value. This suggests that a single surface may be used for hub-to-tip flow field solution and that assigned and computed values of velocity components and fluid properties at any point on this surface must represent a satisfactory circumferential-average for the given x, r coordinates. For the compressor case, flow in each axisymmetric stream tube should be assumed adiabatic but not isentropic.

To support the choice of the axisymmetric and adiabatic stream tube approximation, and to justify continuation of this assumption in the future, both computational and experimental reasons may be given. It has already been noted that iterative S_2 and S_1 stream surface solutions are difficult in a computational sense. Even in cases where totally inviscid flow has been assumed from the beginning (for example, Ref. 62), computation time is substantial for any numerical solution of the full flow field.

From an experimental viewpoint, almost all compressor blade row performance has been measured and reported so as to support the axisymmetric stream tube concept. Circumferential surveys have been made in experiments on axial-flow compressor stages, especially downstream from stationary blade rows, but in almost all cases these data have been reported on a circumferential-average basis. Although instrumentation and procedures for acquiring a detailed quantitative picture of the flow through both rotating and stationary blade rows is now in use in research programs (Refs. 63 and 64), data must be taken and analyzed for a number of representative blade rows in order to give sufficient support to attempts to compute compressor flows on a non-axisymmetric basis.

2. EFFECTIVE BLADE SECTION PROFILE AND CASCADE GEOMETRY

Three possibilities for definition of effective cascade geometry were outlined in Section III. Each method is supported by a rational technical argument and each has been used within the framework of an overall design system to fix the geometric characteristics of rotor and stator blade rows for research and development compressors and fans. Furthermore, these blade rows (for example Ref. 17 and 18) have involved stream surface shapes such that choice of effective geometry is significant. However, there has been no published experimental evidence to show the superiority of one method.

The justification for spanwise cascade projection is largely based on inviscid flow analysis as applied to the theory of swept airfoils. But, in the regions of compressor blade rows where cascade plane

projection has the greatest influence on effective chord length, solidity and section profile, the real flow is affected heavily by fluid shear stresses. It seems realistic to expect that these stresses depend on the actual flow path geometry followed by the axisymmetric stream surface approximations. Therefore in the following sections of this report it is recommended that the cascade element of the overall flow model be based on an effective cascade geometry using dimensions measured on the axisymmetric stream surface approximations. This is consistent with the methods used in Refs. 24 and 45-47. It is suspected (without verification) that when correctly applied there is little difference between stream surface intersection geometry (Refs. 45-47) and conical surface intersection geometry (Refs.48,65) as far as cascade performance estimation is concerned. The recommended symbols and notation reflect this decision.

It was decided that to maintain some continuity with past development, the blade section profile variables recommended for future correlation should be similar to those used in existing turning angle prediction equations. However, to incorporate the more advanced section profiles such as those using arbitrary camber lines, some definition must be extended or modified. The principal parameters recommended are shown for a linear cascade arrangement in Figures 5 and 6. As correlation variables they are listed on Figure 8.

Section profiles designed for use at high entrance Mach number levels may have leading segments with zero or negative camber (e.g. Ref. 46-48)

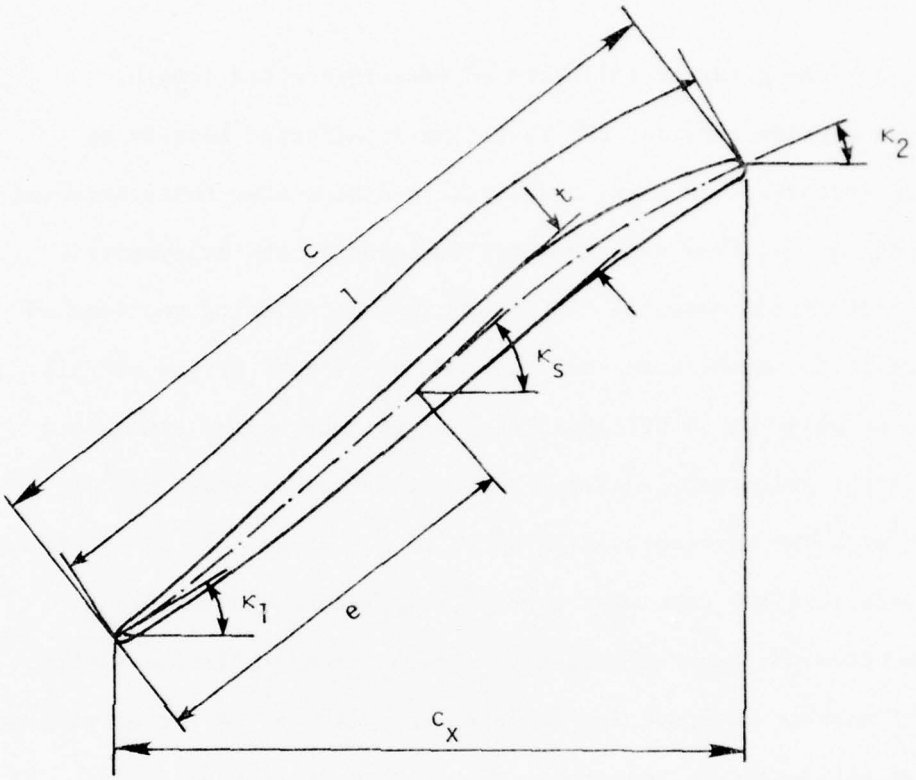

SYMBOL	VARIABLE	RELATED CORRELATION VARIABLE
κ_1	INLET CAMBER LINE ANGLE	κ_1
κ_2	EXIT CAMBER LINE ANGLE	κ_2
LER	LEADING EDGE RADIUS	LER/c
t	MAXIMUM THICKNESS	t/c
TER	TRAILING EDGE RADIUS	TER/c
d	LOCATION OF MAXIMUM THICKNESS (MEASURED ALONG l)	d/l
c	CHORD	c
c_x	AXIALLY-PROJECTED CHORD	c_x
e	INFLECTION POINT	e/c
κ_s	INFLECTION POINT CAMBER LINE ANGLE	κ_s

Figure 8. Recommended Cascade Blade Section Correlation Variables.

and inflection points in the camber line. The sections produced have a "J" or "S" shape. Aside from this the thickness distribution for high entrance Mach number sections is usually characterized by a low maximum thickness/chord line length ratio with the location of maximum thickness in the trailing segment of the section. While zero or negative leading segment camber may have a strong influence on total-pressure losses produced by shock waves, it was believed that the existence of some negative camber has little direct influence on the cascade deviation angle. It is recommended that for blade section profiles with negative camber leading segments, the location of maximum camber should be given as the location in fraction of total chord of the position of maximum positive camber. The section camber angle required for prediction of deviation angle should be determined as the camber angle of the section downstream from the camber line inflection point, as shown in Figure 8. The effective chord length should be considered as the total chord length on the stream surface approximation, as with convential blade section profiles.

For cascade blade sections profiles with zero or positive camber in the leading segment, definitions are unchanged from past practice except for the substitution of camber line length for chord length in the maximum thickness location variables. In cases when a blade section profile may be prescribed without definition of a camber line (for example, Ref. 66), an effective camber line shape can be obtained by construction of a mean line bisecting profile thickness along the length of the section.

Recommended cascade geometry variables for correlation purposes are stagger angle, the angle between the blade chord line and the axial direction, and the solidity

$$\sigma = \frac{c}{\frac{\pi(r_1 + r_2)}{N}} \tag{1}$$

for annular cascades, and

$$\sigma = \frac{c}{s} \tag{2}$$

for linear cascades.

The report section SYMBOLS AND NOTATION gives definitions conforming to the discussion above. It should again be noted that the layout of blade section profiles on any approximation to an axisymmetric stream surface is a matter which requires some attention to detail and the principles of descriptive geometry.

3. CASCADE AERODYNAMIC PERFORMANCE EVALUATION

The primary objective of this investigation was to suggest improved methods for prediction of the flow turning characteristics of blade rows in advanced axial-flow compressors. These methods should be compatible with contemporary compressor design/analysis systems. Both of these requirements admit the possibility for correlation of either relative flow turning angle or deviation angle. The usual argument in favor of deviation angle suggests that it is more suitable for correlation because it does not for a given cascade geometry show a large change as cascade flow inlet angle changes (Ref. 67-69. For continuity it has the advantage

of use over a long period of time in recognized prediction methods (see Section V and Appendices A and B). The following sections consider only the possibility of an improved correlation involving prediction of deviation angle measured from the cascade section profile trailing-edge camber line direction. The other kinematic variables in performance evaluation are selected from those discussed in Section III. 4. These include the cascade entrance fluid angle β_1 measured relative to the blade section on an axisymmetric stream surface approximation, and the incidence angles i_c and i_{ss}. When the possibility exists for data reduction it is recommended that average blade-to-blade flow angles should be obtained on a mass-flow-weighted basis in determination of both deviation and incidence.

While the axial velocity-density ratio Ω has under certain conditions an important influence on deviation angle, it was decided to account for this influence in an indirect fashion through other flow field parameters. The value of Ω as discussed in Section III has the physical significance of a stream tube area ratio, and in the context of the axisymmetric stream tube approximation, it represents the radial stream tube area ratio $r_1\ dr_1/r_2\ dr_2$ for a cascade section in a compressor. The effect of increased Ω is to give a decreased diffuser area ratio across the cascade and a tendency toward reduced cascade loading with reduced adverse static pressure gradients on the blade section surfaces. Inversely decreases in Ω tend to increase diffusion loading and to increase adverse static pressure gradients. The latter effects are those which act in the direction of increasing profile loss.

Where profile losses are discussed in the following sections, these losses are presumed to be associated with a relationship like Equation (7). When experimental cascade data is reduced by the two-dimensional momentum method or any of the procedures which give fully-mixed values of average total pressure (Ref. 50), loss coefficients computed according to Equations (3) to (5) are total coefficients including mixing and shock losses. As pointed out in Ref. 58 and elsewhere a substantial portion of the published systematic cascade data reports essentially fully-mixed loss parameter values. This should be recalled when comparison are being made.

SECTION V

EXISTING DEVIATION/TURNING ANGLE PREDICTION EQUATIONS

Three principal correlation equations are used as the bases for prediction of changes in relative flow angle across compressor blade rows. The initial development of all of these correlations occurred before 1960, and there has been little substantive change in the base equations since that time. All of the equations are semi-empirical in nature, with an analytical background supported by the results of linear cascade experiments. As a consequence of the theoretical and experimental flow field conditions associated with all three deviation/turning angle correlations, certain real compressor blade row problems are not resolved by the basic procedures:

1) Stream surface radial location, radius change and shape are not linear cascade variables. The problem of effective blade section profile definition does not occur (see Section II).
2) Changes in radius do not affect blade spacing or effective chord length determination. Problems of cascade geometry definition do not occur.
3) Stream tube effective area changes are not prediction equation variables. Axial velocity-density ratio (Ω) was assumed equal to 1.0 for analysis and experiments used to generate the correlations, or it was considered not to be a strong influence on the results (see Section III).
4) The prediction methods are directed toward the selection of suitable cascade geometry combinations for design point

operation in conservative, non-extreme compressor configuration. There is insufficient theoretical or experimental support in terms of marginal loading levels and setting angle-solidity combinations.

The conditions associated with the initial development of the three deviation/turning prediction methods are considered sufficiently important to justify a separate descriptive subsection and an Appendix devoted to each one. The Appendices also collect in one location material drawn from numerous sources which are sometimes difficult to locate. The Appendices are organized so that the restrictive conditions connected with each correlation are given in a standard format. Naturally in the application of the basic correlations to the design or analysis problems for real compressor blade rows, strategies have been developed to adapt the definitions of equation variables to compressor geometry and to extend the ranges of geometric and aerodynamic variables outside the limits suggested by the base correlations. Each Appendix contains some examples illustrating these strategies.

It should be remembered that the objective in the case of each deviation/turning angle method was to permit estimation of the change in average relative flow direction across a cascade arrangement operating in a two-dimensional flow at specified entrance flow conditions including a defined entrance flow direction or incidence angle. The base incidence angle was different for each correlation, was not intended to represent a design incidence, and was indicative only of prevailing ideas concerning favorable aerodynamic operation.

1. NATIONAL GAS TURBINE ESTABLISHMENT (NGTE) CORRELATION

The overall development of axial-flow compressor design methods in the United Kingdom during the period 1939 to 1950 included research leading to the NGTE deviation angle prediction equation, commonly called Carter's rule. Figure 9 shows the primary pattern of development of the correlation by reference to supporting analysis and experiments.

The NGTE correlation was based on trends in deviation angle predicted by analysis of two-dimensional potential flow through cascades with sharp trailing-edge blade sections to permit use of the Kutta-Joukowski circulation condition. This analysis was supported and the equation for deviation was adjusted by the results of plane cascade experiments. The correlation was initially proposed to give the deviation angle corresponding to a nominal flow turning angle, equal to 0.8 times the turning measured at cascade stall (maximum turning). In the theoretical studies the base incidence was either arbitrarily defined (Ref. 74, i_c = 4 deg) or set at the value for maximum lift/drag ratio (Ref. 75). In Appendix A the i_{opt} values of Ref. 75 were considered to be the base incidence. This Appendix summarizes the background and subsequent application of the NGTE deviation method.

In the recommended terminology of this report, the base equation of the NGTE correlation is

$$\delta = \frac{m_c \varphi}{\sqrt{\sigma}} \tag{14}$$

Reference 75 also included generalized performance curves to permit prediction of cascade turning angles for non-optimum incidence.

2. NATIONAL ADVISORY COMMITTEE FOR AERONAUTICS/NATIONAL AERONAUTICS AND SPACE ADMINISTRATION (NACA/NASA) CORRELATION

The NACA/NASA procedure for estimation of deviation angles for axial-flow compressor cascades was developed at the Lewis Flight Propulsion Laboratory of the NACA between 1952 and 1956 as a part of the preparation of a summary of NACA compressor design technology.

The NACA/NASA correlation used previous theoretical work (Refs. 76 and 77) as well as the NGTE correlation to suggest the form of the base equation, but specifically attempted to recognize and eliminate deficiencies noted in the NGTE method:

1. The NGTE correlation predicts zero deviation angle for zero camber blade section profiles. Both theoretical and experimental studies indicated a non-zero deviation angle for two-dimensional flow across staggered cascades with zero camber and non-zero thickness at zero incidence.
2. Both camber line shape and blade section thickness distribution were believed to significantly affect deviation angle.
3. Use of a constant exponent on the solidity parameter in the NGTE correlation was considered unsatisfactory.

In the recommended notation of this report the NACA/NASA correlation equation is (Ref. 67).

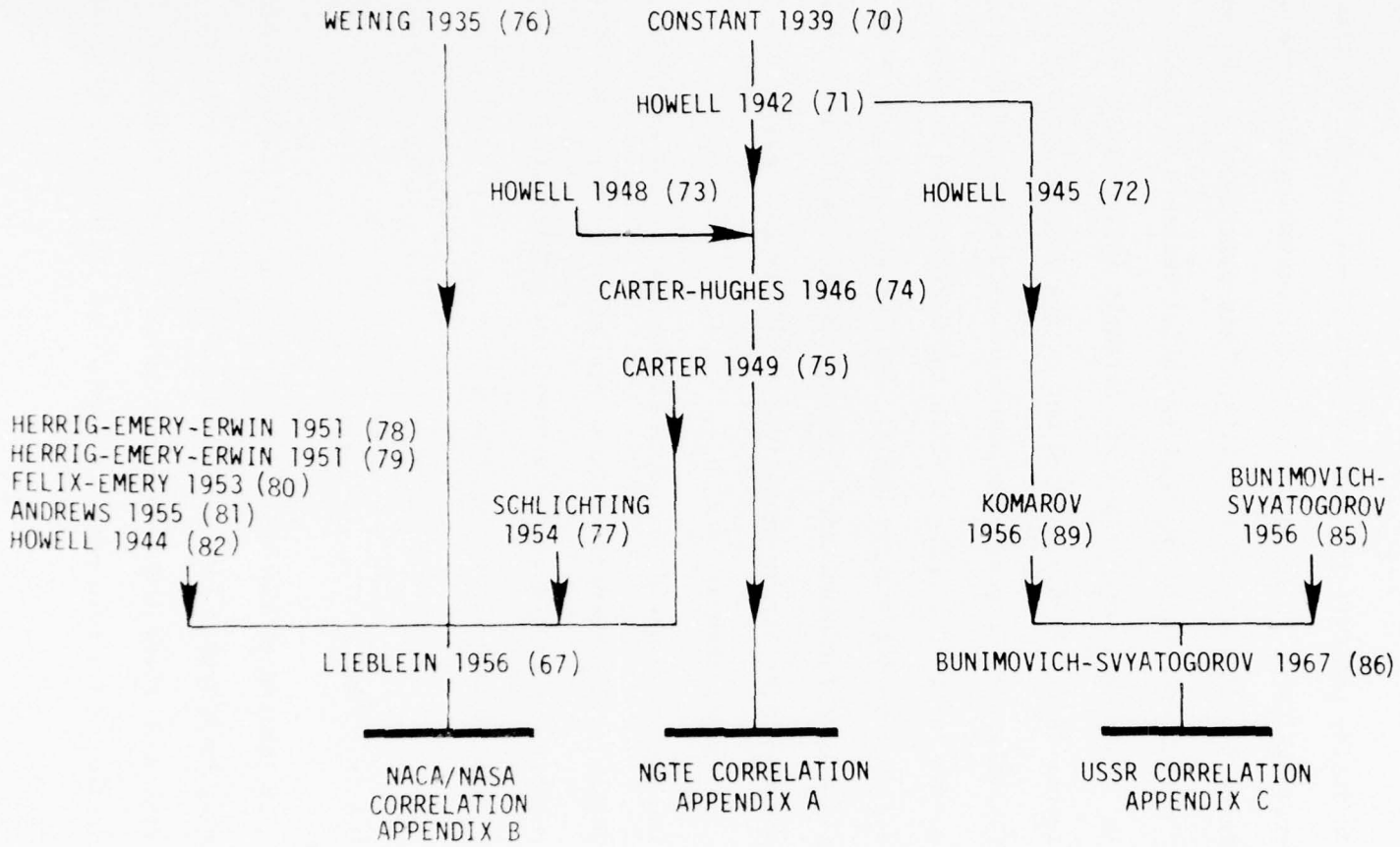

Figure 9. Pattern of Development of Deviation/Fluid Turning Angle Correlations. Numbers in Parentheses are Reference Numbers.

$$\delta_{ref} = \delta_o + \frac{m_{\sigma = 1}}{\sigma^b} \varphi \qquad (15)$$

To define the correlation, available plane cascade experimental data were evaluated to isolate a base of experiments which could be considered two-dimensional ($\Omega = 1.0$). This eliminated a substantial number of sources, including most potential variants in blade section profile. The final correlation was strongly influenced by NACA experiments (Refs. 78-81) carried out at low cascade inlet Mach numbers. Unfortunately these experiments also were sequences of data points at constant inlet flow angle β_1 with the variation in incidence obtained by changing stagger angle. This created difficulty in defining a base incidence angle related to the operation of real compressor cascade arrangements, where the stagger remains constant as inlet flow angle changes (Ref. 83).

The predicted deviation angle corresponds in the NACA/NASA correlation to a reference minimum loss incidence angle at low inlet Mach numbers. A procedure was derived for determining the effects of incidence changes. The equation is

$$\delta = \delta_{ref} + (i - i_{ref}) \left(\frac{d\delta}{di}\right)_{ref} \qquad (16)$$

but it is limited to the relatively small range of incidence at low inlet Mach number in which the slope $\left(\frac{d\delta}{di}\right)_{ref}$ is constant.

Figure 9 shows the development pattern of the NACA/NASA correlation, and a more complete summary of its content is given in Appendix B.

3. USSR CORRELATION

This correlation is the product of extensive systematic plane cascade experiments performed in the Soviet Union between 1951 and 1956. Two independent sets of data are involved (Ref. 84 and 85), reporting results for cascade entrance Mach numbers up to 0.92 with Ω in the range 1.0 to 1.15 (not controlled).

The correlations developed (Ref. 86) are almost entirely empirical in nature, but they cover a wide range of cascade blade row geometry and substantial variations in blade section profile, unfortunately only including two camber line shapes with very limited movement of the position of the maximum camber location.

The principal prediction equation estimates the low-speed flow turning angle corresponding to two-dimensional flow across a cascade operating at an optimum incidence angle. In this case the optimum incidence is based on the minimum value in the loss-incidence curve at a specified high-subsonic Mach number level (Ref. 85). A relatively simple equation is suggested for the prediction of optimum incidence.

In the recommended notation of this report

$$\Delta\beta_o = \left[\frac{(\Delta\beta_o)_{d/c}}{(\Delta\beta_o)_{d/c = 0.4}}\right]\left[\frac{(\Delta\beta_o)_{t/c}}{(\Delta\beta_o)_{t/c = 0.10}}\right]\left[\frac{K\varphi}{1000} + B\right] \quad (17)$$

$$K = \left(5 - \frac{2}{\sigma}\right) \sqrt{(90 - \gamma)^2 - \frac{1000}{\sigma}} + 100 \left(5.5 - \frac{2.6}{\sigma}\right)$$

$$B = 8 \left(\frac{1}{\sigma}\right)^2 - \frac{17}{\sigma} + 16$$

$$\frac{(\Delta\beta_o)_{d/c}}{(\Delta\beta_o)_{d/c = 0.4}} = 1 - 0.28 \, (d/c - 0.4) \text{ for } \frac{d}{c} = 0.3 \text{ to } 1.0 \qquad (18)$$

$$\frac{(\Delta\beta_o)_{t/c}}{(\Delta\beta_o)_{t/c = 0.10}} = 1 - 1.6 \, (0.10 - t/c) \text{ for } \frac{t}{c} = 0.0125 \text{ to } 0.125$$

(19)

Generalized curves are given in Ref. 85 for the influence of cascade entrance Mach number and incidence variation above and below optimum on cascade fluid turning angle $\Delta\beta_o$. Appendix C outlines the basis for the USSR correlation. Little is known about specific applications.

SECTION VI

DEVIATION ANGLE CORRELATION FOR ADVANCED FAN AND COMPRESSOR DESIGN/ANALYSIS

1. EXPERIMENTAL DEVIATION/TURNING ANGLE DATA

a. Plane Cascade Data

Figure 9 shows that a very limited part of the linear cascade data available in the literature has been used in development of the principal existing deviation/fluid turning angle correlations. In the majority of linear cascade experiments carried out before 1950, the results were not suitable for correlation because of unsatisfactory control of aerodynamic variables in the test programs and because of inadequate measurement and data reduction methods (refs. 67,87). However, after 1950 and up to the present, numerous linear cascade facilities have been used for experiments with both subsonic and supersonic inlet flow through compressor blade section profiles in cascade arrangement. Of the published results of experiments conducted during the past 25 years, some but not all might be satisfactory for extension or development of deviation/turning angle prediction methods. Certain preconditions should be considered in evaluation of the data:

1) Is the blade section profile and cascade geometry adequately described for definition of geometric variables?

2) Have the independent aerodynamic variables been satisfactorily controlled, so that the parameters influencing fluid turning angles can be considered numerically reliable?

3) Are the measurement and data reduction methods clearly described so that the basis of numerical values of both deviation/turning angle and total-pressure loss parameters can be understood?

4) Is there sufficient data available to assist in extension of the range of applicability of existing correlation forms or to support the development of a new prediction method?

A large number of data sources were investigated during the present study and in the case of linear cascade results several sets of published data were considered suitable in terms of most of the above criteria. These include Refs. 58, 59, 66, 80 and 88-103. In addition, some unpublished data was obtained. In general both the published and unpublished results met all requirements except for number 4 above. While the data has been acquired in order to meet a limited research or development objective, it is not systematically planned so as to allow the generation of a new prediction method.

b. Fan and Compressor Cascade Configuration Data

Annular cascade results from flow passage surveys in rotor and stator rows of axial-flow fans and compressors are not available in significant quantities, especially where the data quality is adequate for possible correlation. A large number of reported and unpublished test data sets were considered as candidates, with the vast majority of these sets from rotor and stage experiments carried out by the NASA and by NASA contractors.

The principal question of data adequacy for deviation/turning angle and loss correlation exists as a result of the presence of part-span dampers or shrouds in the rotor blade rows involved. While the damper geometries do not reduce the value of the data for many purposes, the aerodynamic effects cover enough of the flow passage downstream from the shrouded row to confuse the data for angle and loss correlation (Ref. 104). Probable exceptions exist in the case of Refs. 18 and 105-108, and possible additional sets may be evaluated as satisfactory in the future (e.g. Refs. 109-112).

Some reservations must exist concerning the use of fan and compressor passage survey data measured with conventional pressure and temperature probes. The data-averaging characteristics of many probe types remain in question. The utilization of optically-measured flow passage data is discussed later in this section.

2. PROPOSED METHOD FOR DEVIATION ANGLE CORRELATION

a. Correlation Equation Form

Study of the existing deviation/fluid turning angle correlations and the data described earlier in this section shows that beyond the questions related to data quality, both geometric and aerodynamic questions remain. Because of gaps in coverage of the available data it was decided that the immediate objective should be limited to modification of an existing correlation method. It was shown in Appendices A and B that the NGTE deviation correlation has been applied to design of actual compressor configurations more frequently than the NACA/NASA correlation. Furthermore, although the NACA/NASA correlation accounts directly for more blade section profile variables, the accounting has been questioned (Ref.68) and modification might be difficult because of the correction coefficients used. The extremely empirical form of the USSR fluid turning angle correlation was thought to make it unsatisfactory for modification although the trends shown are significant and worthy of study.

Based on the preceding reasoning, it was decided to suggest modification of the NGTE correlation equation from its original form

$$\delta = \frac{m_c \varphi}{\sqrt{\sigma}} \qquad (14)$$

In the original form the equation is quite limited in terms of both cascade geometry and aerodynamic variable range. The principal geometric variable affecting deviation angle that is not satisfactorily accounted for is the position of maximum camber a/c. Ref. 48 suggests the substitution of an equation for m_c of the form

$$m_{cm} = (0.219 + 0.0008916\gamma + 0.00002708\gamma^2) \times \left(\frac{2a}{c}\right)^{2.175 - 0.03552\gamma + 0.0001917\gamma^2} \quad (20)$$

The experimental support for this modified m is not clear, but the trends associated with its use are similar to those of other application modifications. It should be noted that the definition of the angle γ given in ref. 48 is slightly different from that used in this report and in the NGTE correlation. This difference is not considered material.

Possible additional geometry-related changes in the equation might correct for maximum profile thickness location and value. Such corrections were included in the NACA/NASA equation and the USSR correlation. However, the data available on thickness effects is not conclusive and is related to aerodynamic variables (ref. 113). No modification is proposed here. No equation modification is suggested for the constant exponent 0.5 on the solidity parameter. Variable exponents have been used in other correlations, for example the NACA/NASA equation.

Aerodynamic variables of possible importance in modification are the cascade inlet Mach number, Reynolds number, turbulence

properties, axial velocity-density ratio and in an overall sense the level of diffusion loading.

Because all three of the original correlation forms in common use were based on initial estimation of deviation/turning angle for low speed, two-dimensional flow at Reynolds numbers above a critical level, these possible modifications assume great importance. In many compressor design/analysis applications the strategy selected has been to suggest separate correlation procedures for the individual variables. This is not only a technically complex strategy but it also leads to possible discrepancies caused by the interaction of the aerodynamic variables. For example, some early studies of the effect of axial velocity-density ratio on deviation angle indicated a simple relation between axial velocity ratio and deviation of the form

$$\delta = \delta_{AVR=1.0} - 10(AVR - 1.0) \qquad (21)$$

Subsequent experiments (Ref. 96-103) quickly demonstrated that equation 21 was not general and that for low cascade diffusion parameter levels axial velocity ratio changes have little effect on deviation angle. As a consequence the development of separate correction mechanisms for individual aerodynamic variables was questioned and discarded as a feasible alternative.

This investigation suggests a departure from the usual approach by noting the correction of deviation angle with boundary layer development on the blade surfaces. This general procedure has already been used where the NGTE equation has been applied with the actual fluid turning angle replaced by the equivalent circulation value (Appendix E).

However, it was decided that a more direct connection with the real flow conditions might be possible and advantageous.

It has already been observed that there are two experimentally-supported prediction elements in a current compressor design system. The requirement for deviation/fluid turning angle estimation is no more significant than the requirement for prediction of losses. Losses are ordinarily considered in terms of components described as profile losses, shock losses, secondary losses and mixing losses. The scope of this report does not permit a detailed review of this classification, but it is necessary to note that trailing edge deviation angle in a cascade is directly or indirectly dependent on the character of each of the loss components except for the mixing losses which occur in the region downstream from the trailing edge.

During the course of this study it was noted that principal regions of discrepancy between the results of linear cascade experiments and the three base deviation/turning angle correlations occurred in the operating regimes associated with substantial diffusion loading and high profile losses. This was not an original discovery, since the developers of both the NGTE and NACA/NASA correlations recognized clearly the failure of the prediction equations for high cascade diffusion parameter levels. As a result some consideration was given to suggestion of a correlation modification related to a profile loss parameter such as $\bar{\omega} \cos \beta_2/2\sigma$ or θ^*/c (refs. 61, 113). However, it was noted that such an approach would have to be limited by the fact that increases in profile loss do not necessarily indicate large increases in deviation angle, especially at non-optimum incidence. Figure 10 shows this clearly at low incidence angles.

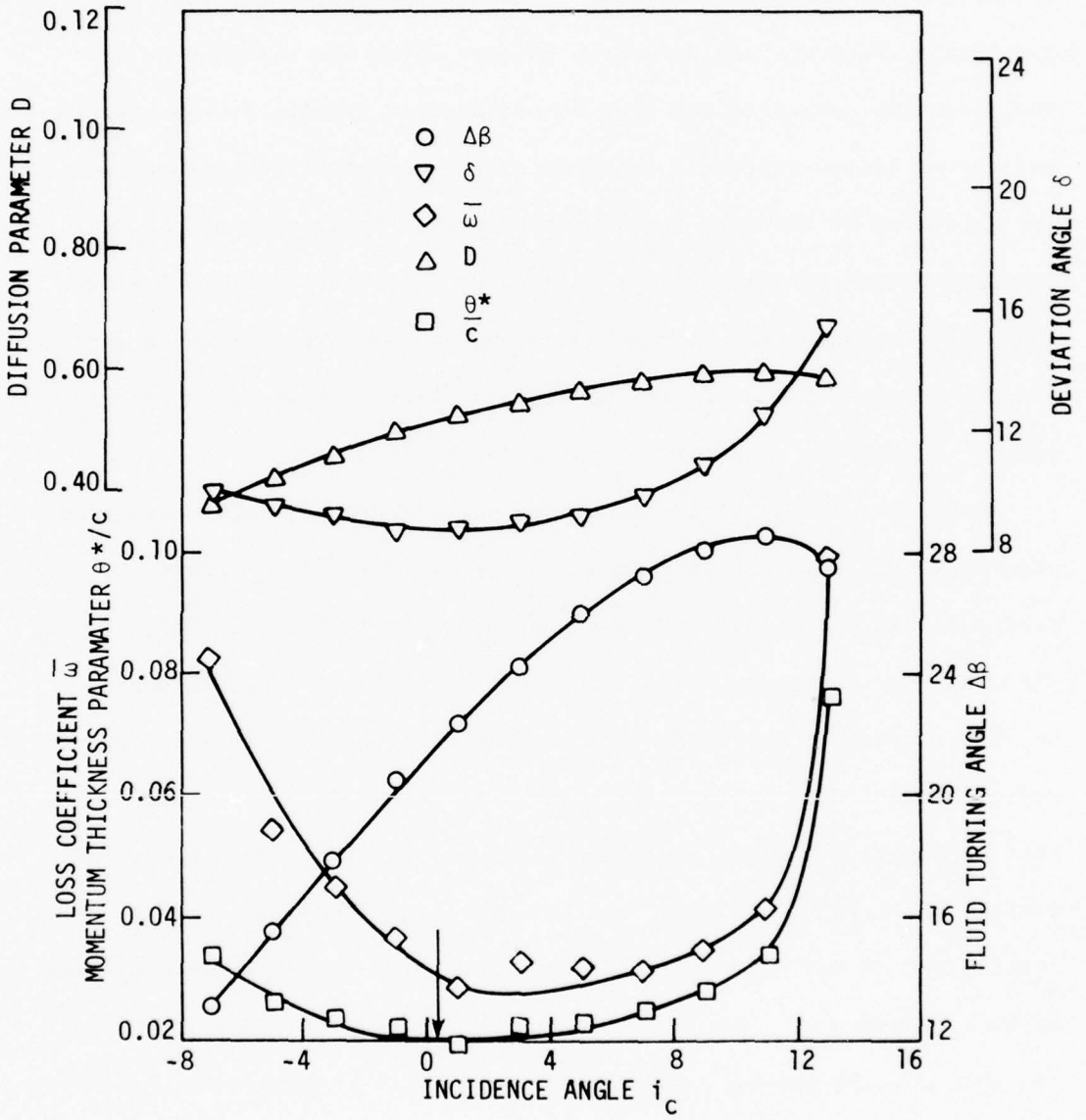

Figure 10. Experimental Data for Plane Cascade, NACA 65-($12A_{10}$)10 Blade Section Profile at β_1 = 60 deg and σ = 1.50 (Replotted from Ref. 78).

Examination of the trends in deviation angle shown by the existing linear and annular cascade results leads to the conclusion that the numerical values are influenced by factors which are relevant to inviscid flow concepts, but that beyond certain loading levels viscous influences become extremely important. The inviscid flow influences are evidenced by the fact that the theoretical background of the NGTE prediction equation is entirely related to inviscid flow computations. However, the connection between viscosity and deviation angle is also obvious because of the effects of blade surface boundary layer development on velocity patterns in the blade-to-blade flow.

Historically the blade surface boundary layer has been considered principally in terms of its connection with profile loss values. Numerous analyses relate to this problem (Refs. 52,53,55,61,114), where the quantitative connection of boundary layer with loss parameters has been through combined suction surface and pressure surface boundary layer parameters at the trailing edge. Values of δ^*/c, θ^*/c and H have been utilized which represent the total of suction and pressure surface conditions. However, in the case of deviation angle, the development of the suction surface boundary layer considered independently appears to assume the greatest importance. This has a logical physical explanation. If the suction surface boundary layer grows, the blade-to-blade passage flow will be influenced so as to give higher deviation angles. If the boundary layer separates or the separation point moves forward still higher deviation will result. In contrast, growth of the pressure surface boundary as observed in compressor cascades is

normally limited and its effect on the blade-to-blade flow would in any case be to suppress deviation.

As an initial step in the modification of the NGTE correlation equation, it is proposed that terms or multipliers should be added which recognize specifically the factors which control the growth of the suction surface boundary layer and its condition with respect to separation. The parameter Deq suggests itself as a component of the modification, since numerical values of Deq correlate quite well with suction surface boundary layer growth and separation trends. Heilmann (refs. 102,103) has shown that the effect of axial velocity-density ratio on deviation angle is not large if the diffusion loading levels are below a limiting value but that as the loading level increases the effect becomes very significant. An equation form

$$\delta = m_{cm} \frac{\varphi}{\sqrt{\sigma}} \left[fcn\left(\frac{Deq}{Deq,base} \right) \right]$$

is suggested with the function fcn(Deq/Deq, base) to be determined from the data.

A more direct relationship between individual boundary layer parameters for the blade section suction and pressure surfaces and the deviation angle would be a better solution to the modification problem but is is unlikely that this can be accomplished without some analysis as well as additional data. This would also allow the effects of Mach number and Reynolds number on boundary layer development and on deviation angle to be included in a more satisfactory manner.

b. Required Additions to Data Base

To permit a thorough test of the relationship between blade surface boundary layer parameters and the deviation angle as well as for the evaluation of boundary layer computation systems in the blade-to-blade flow field environment it is necessary that experimental data be obtained in the blade surface regions of blade-to-blade stream tube approximations. Data should be obtained for both subsonic and supersonic entrance conditions in a few linear cascade geometries typical of current compressor configurations. These data would be useful as test cases for many purposes in addition to that of supporting a new deviation angle correlation. Values of δ^*, θ^* and H should be known through as much of the passage as possible for both suction and pressure surface boundary layers.

In order to provide further support for correlation, data should be obtained within blade rows of fans and compressors. This information is needed to give a better basis for design system computations on both hub-to-tip and blade-to-blade solution surfaces. Figure 11 shows an example distribution of relative flow angle on a blade-to-blade stream surface approximation as measured by the dual-beam laser method. It is clear that some careful analysis is required to determine correct procedures for calculating the correct average or effective flow angle at various locations in the blade channel if a single hub-to-tip calculation surface is used for compressor design/analysis.

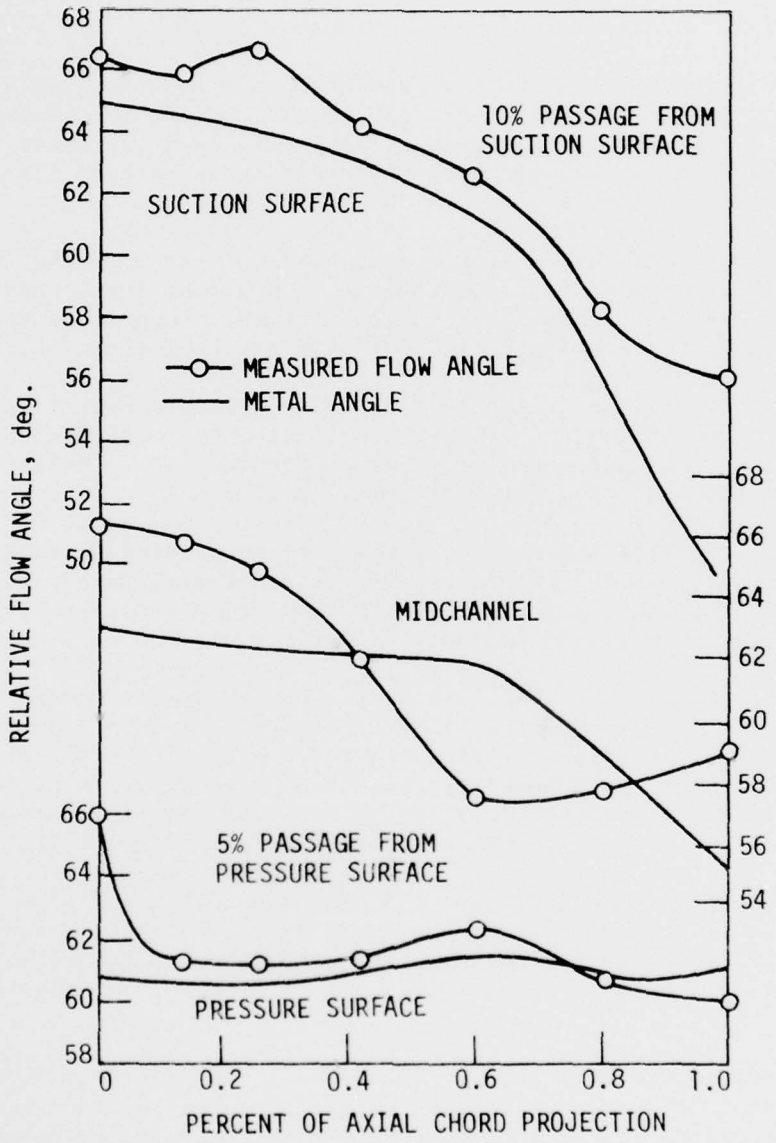

Figure 11. Distribution of Relative Flow Angle in Rotor Blade Row of Transonic Compressor Stage Operating at Design Speed and Maximum Efficiency Flow Rate. Radial Location 89 Percent of Blade Height from Hub. (Data Courtesy of H. B. Weyer and R. Dunker, DFVLR - Köln).

SECTION VII

CONCLUSIONS

The results of this investigation indicate that:

1) The three principal methods for prediction of deviation angle and relative fluid turning angle for compressor and fan blade sections in cascade arrangement are currently used for blade section profiles and in aerodynamic variable regimes far outside the original correlation limits.

2) There is not enough experimental data available from either linear cascade or compressor test programs to support the development of a new correlation. Therefore, in the immediate future the most reasonable approach would be to modify an existing correlation.

3) The deviation angle correlation originally proposed by the National Gas Turbine Establishment (NGTE) has received the most frequent application to compressor configuration design. It is believed to represent the best candidate for modification.

4) Failure of the NGTE and other correlations to predict deviation angle correctly is the result of effects of several aerodynamic parameters interacting in the viscous flow region near the blade surfaces, principally on the suction surface.

5) In addition to the variables which influence deviation angle in cases where inviscid flow is assumed (camber, blade section profile, stagger angle, solidity, incidence), the features of the real flow field which have the most direct effect on the magnitude of deviation angle are the characteristics of the blade suction surface boundary layer and not necessarily the level of total profile loss.

6) One parameter which correlates well with the growth and separation tendencies of the suction surface boundary in compressor cascades is the diffusion loading parameter Deq. A term including this parameter is suggested as an addition to the NGTE correlation equation.

7) An objective of future research should be to acquire data which defines separately the characteristics of the suction and pressure surface boundary layers for compressor blade cascade arrangements. This data is necessary to permit the development of generalized deviation/turning angle prediction methods.

APPENDIX A

NATIONAL GAS TURBINE ESTABLISHMENT DEVIATION ANGLE CORRELATION[1]

Base Equation

$$\delta = m\Theta\sqrt{\frac{s}{c}} \qquad \text{(Ref. 75)}$$

at

$$i = i_{opt} \qquad \text{(Ref. 75)}$$

δ deviation angle, angle between cascade exit average fluid angle and line tangent to blade section camber line at trailing edge, degrees

m function of blade section stagger angle and camber line shape, Figure A-3.

ζ blade section stagger angle, angle between chord line and axial direction, degrees

Θ blade section camber angle, angle between lines tangent to section camber line at leading and trailing edges, degrees

s blade spacing, tangential distance between equivalent points on adjacent blade sections

c chord length, length of straight line connecting points where camber line intersects leading and trailing edges

i incidence angle, angle between cascade inlet average flow angle and line tangent to blade section camber line at leading edge, degrees

[1] Symbols and notation defined in Appendix A correspond to original publication of correlation except for sign convention on stagger angle. See also Figures A-1 and A-2.

i_{opt} incidence angle predicted to give maximum lift/drag ratio for given cascade geometry, degrees

α_1' blade section camber line angle at leading edge, measured from axial direction, degrees

α_2' blade section camber line angle at trailing edge, measured from axial direction, degrees

α_1 average fluid angle at cascade inlet, measured from axial direction, degrees

α_2 average fluid angle at cascade exit, measured from axial direction, degrees

ε fluid turning angle, degrees

V_1 fluid velocity at cascade inlet

V_2 fluid velocity at cascade exit

Base Airfoil Section Profiles

C.1 (Ref. 71)

C.2 (Ref. 71)

C.4 (Ref. 82)

Base Camber Line Shapes

Circular-arc (Ref. 71)

Parabolic, $\frac{a}{c} = 0.40$ only (Ref. 71)

Base Cascade Geometry Limits

$\frac{a}{c}$ { 0.50 circular-arc camber line
0.40 parabolic camber line

$\frac{d}{c}$ { 0.33 C.1 section; 0.30 C.2 section; 0.30 C.4 section

$\frac{t}{c}$ Ref. 75 based on analysis and data for t/c = 10%

LER { 0.08t C.1 section; 0.12t C.2 section; 0.12t C.4 section

TER { 0.02t C.1 section; 0.02t C.2 section; 0.06t C.4 section

ζ m defined for ζ from 0 to 60 deg

$\frac{s}{c}$ Ref. 75 based on data for $\frac{s}{c}$ from 0.5 to 1.5

Θ Applicable camber limited by section loading

Base Aerodynamic Variable Range

M_1 analysis-incompressible flow

results used in Ref. 75 all were for low-speed plane cascade flow

Re results used in Ref. 75 refer to effective Re of about 4×10^5 based on chord and exit velocity

Ω Ω = 1.0, two-dimensional flow assumed in analysis and experiments

Turbulence data not available

Design/Analysis Application Examples

A. Modified Base Equation and Incidence

The NGTE rule has been used to predict deviation angle for a range of incidence levels when cascade diffusion loading is low. This is done on the assumption that deviation variation with incidence is not large when profile losses are low.

Various investigators including Refs. 20, 69 have given equations for m based on Fig. A-3.

Application of the NGTE rule to design has frequently included a capability to add an arbitrary angle correction (for example, Refs. 17, 48).

Ref. 18 applied a modified equation to design

$$\delta = \frac{(\varepsilon - i)\, m_c \sqrt{\frac{s}{c}}}{1 - m_c \sqrt{\frac{s}{c}}}$$

with

$$m_c = 0.92 \left(\frac{a}{c}\right)^2 + 0.002\, \alpha_2$$

B. Extended Blade Section and Cascade Geometry Limits

Airfoil Section Profiles and Camber Line Shapes

The NGTE rule has been used for NACA 65-series profiles on circular-arc camber lines (Ref. 69) and for double-circular arc and multiple-circular-arc (DCA and MCA) profiles (Refs. 16, 17, 18, 22). It has been applied to a polynomial camber line with a polynomial thickness distribution (Ref. 115).

Ref. 48 includes an NGTE rule option for the sections defined in that report.

Cascade Geometry Limits

$\frac{a}{c}$ - Equations or curves for prediction of deviation for a/c values less than 0.4 and greater than 0.5 are given in Refs. 17, 18, 22, 48 and 115.

ζ - m values extrapolated by equation to $\zeta > 60$ deg

Blade-To-Blade Surface Radius Change

The NGTE rule has been used for radius change and $\Omega \neq 1.0$ cases by substituting an equivalent circulation turning angle into an equation of the form (recommended notation)

$$\delta = \frac{\beta_1 - i - \beta_{2e}}{\frac{\sqrt{\sigma}}{m} - 1}$$

This approach is used in Refs. 17, 22, 48 and 69. See Appendix E.

C. Extended Aerodynamic Variable Range

M_1 - rule used without M_1 correction for supersonic entrance flows in Refs. 16, 17, 18, 22, 115.

Re - correction suggested in Refs. 70, 71, 72.

Ω - see the method under radius change above and in Appendix E. This approach used in Refs. 17, 22, 48 and 69.

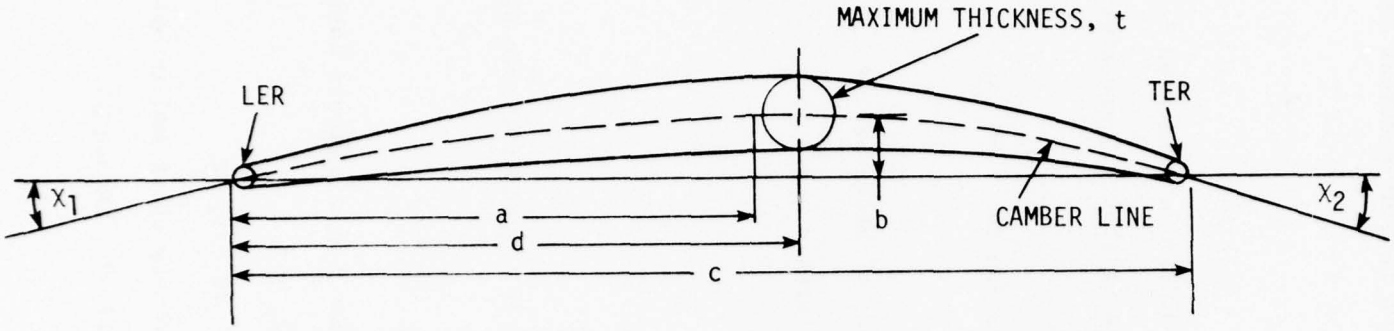

a = LOCATION OF MAXIMUM CAMBER
b = COORDINATE OF MAXIMUM CAMBER
c = CHORD LENGTH
d = LOCATION OF MAXIMUM THICKNESS
LER = LEADING EDGE RADIUS
TER = TRAILING EDGE RADIUS
χ_1 = ANGLE BETWEEN LINE TANGENT TO BLADE SECTION CAMBER LINE AT LEADING EDGE AND CHORD LINE, DEGREES
χ_2 = ANGLE BETWEEN LINE TANGENT TO BLADE SECTION CAMBER LINE AT TRAILING EDGE AND CHORD LINE, DEGREES

Figure A-1. NGTE Blade Section Profile Terminology (Refs. 71 and 75).

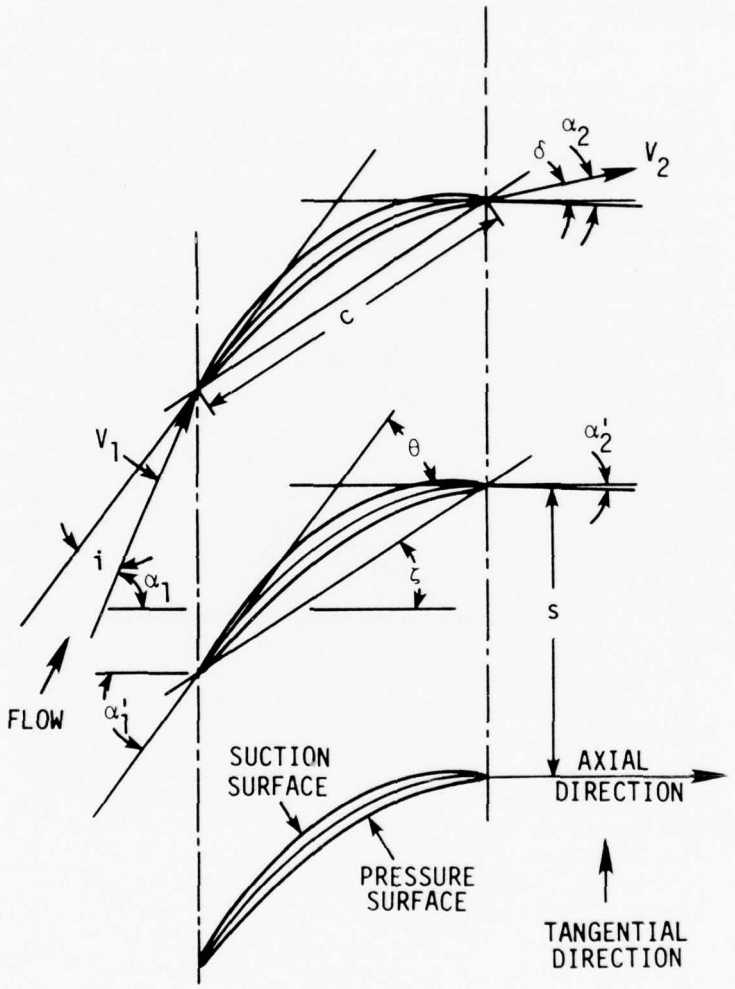

$i = \alpha_1 - \alpha'_1$ $\qquad \theta = \alpha'_1 - \alpha'_2$

$\delta = \alpha_2 - \alpha'_2$ $\qquad \varepsilon = \theta + i - \delta$

$\varepsilon = \alpha_1 - \alpha_2$

Figure A-2. NGTE Cascade Terminology (Refs. 71 and 75).

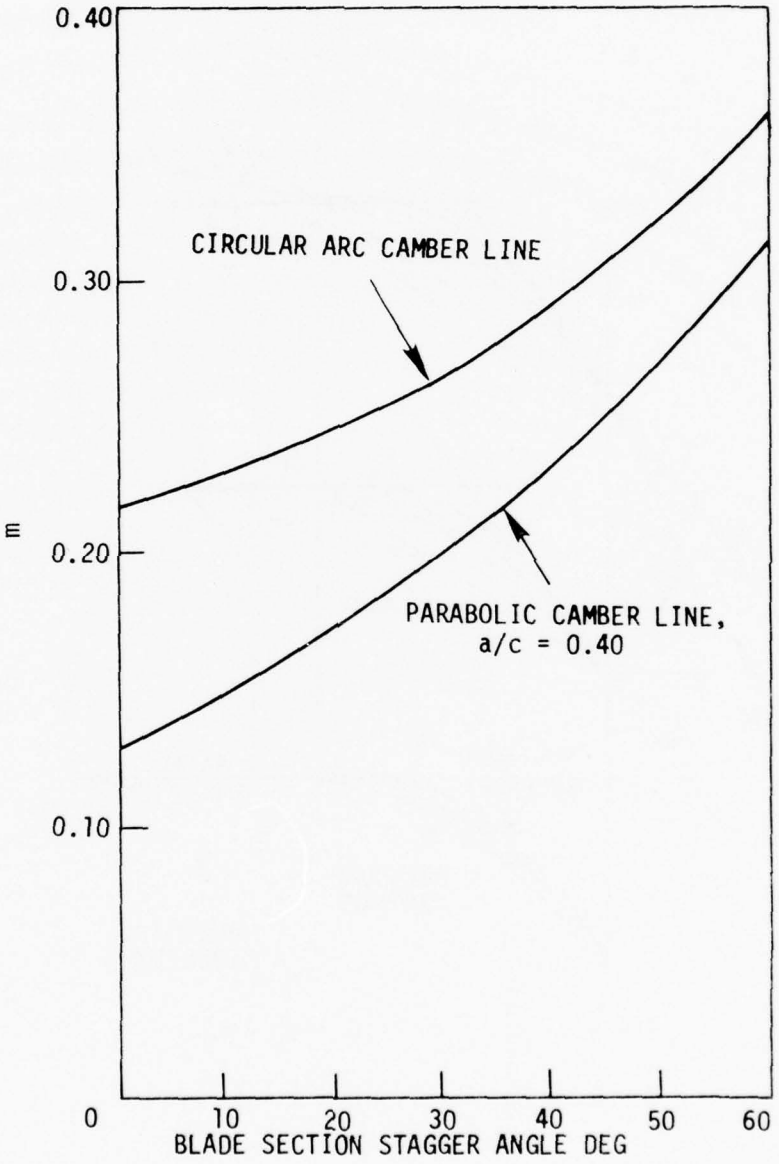

Figure A-3. Coefficient m for NGTE Deviation Angle Correlation [Ref. 75].

APPENDIX B

NACA/NASA DEVIATION ANGLE CORRELATION[1]

Base Equation

$$\delta_{ref} = \delta_o + \frac{m_{\sigma = 1}}{\sigma_b} \varphi \qquad \text{see Figures B-5, B-6, B-7 and Ref. 67}$$

with

$$\delta_o = (K_\delta)_{sh} \; (K_\delta)_t \; (\delta_o)_{10} \qquad \text{see Figures B-3, B-4}$$

at

$$i = i_{ref} \qquad \text{(Ref. 67)}$$

δ_{ref} cascade exit average deviation angle measured from tangent to blade trailing edge camber line direction for cambered cascade, degrees

δ_0 deviation angle measured from camber (chord) line for zero camber cascade with same fluid inlet angle and solidity as the cambered cascade, degrees

$(\delta_0)_{10}$ value of δ_0 for cascade with NACA 65-series blade section airfoil profile and maximum section thickness 10% of chord length, degrees

---

[1]Symbols and notation defined in Appendix B correspond to original publication of correlation. See also Figures B-1 and B-2.

$(K_\delta)_{sh}$ dimensionless correction factor to $(\delta_0)_{10}$ for effects of blade section profile not NACA 65-series

$(K_\delta)_t$ dimensionless correction factor to $(\delta_0)_{10}$ for effects of blade section maximum thickness not 10% of chord length

φ blade section camber angle, with equivalent circular arc camber angle used for NACA A_{10} camber line shape, degrees

σ cascade solidity, ratio of blade section chord length to blade-to-blade spacing or pitch

$m_{\sigma=1}$ rate of change of deviation angle with camber angle for cascade with solidity of 1.0

b correction exponent accounting for variable influence of solidity on δ-φ slope associated with different fluid inlet angles

s blade spacing, tangential distance between equivalent points on adjacent blade sections

c chord length, length of straight line connecting points where camber line intersects leading and trailing edges

i incidence angle, angle between cascade inlet average flow angle and line tangent to blade section camber line at leading edge, degrees

i_{ref} reference minimum-loss incidence angle, degrees (Ref. 67)

κ_1 blade section camber line angle at leading edge, measured from axial direction, degrees

κ_2 blade section camber line angle at trailing edge, measured from axial direction, degrees

β_1 average fluid angle at cascade inlet, measured from axial direction, degrees

β_2 average fluid angle at cascade exit, measured from axial direction, degrees

$\Delta\beta$ fluid turning angle, degrees

V_1 fluid velocity at cascade inlet

V_2 fluid velocity at cascade exit

Base Airfoil Section Profiles

NACA 65-010 blower blade section (on NACA A_{10} camber line only)

C-series airfoil section thickness distributions (on circular-arc camber line only)

Double circular arc airfoil sections

Base Camber Line Shapes

NACA A_{10} (a = 1.0)

Circular Arc

Base Cascade Geometry Limits

$\frac{a}{c}$
- 0.50 NACA A_{10}
- 0.50 circular arc

$\frac{d}{c}$
- 0.30-0.33 C-series
- 0.40 65-010 blower blade section
- 0.50 double circular arc

$\frac{t}{c}$
- $(K_\delta)t$ given in range 0 to 0.12

LER $\begin{cases} 0.0067c & \text{65-010 blower blade} \\ 0.08 \text{ to } 0.12t & \text{C-series} \end{cases}$

TER $\begin{cases} 0.0015c & \text{65-010 blower blade} \\ 0.02 \text{ to } 0.06t & \text{C-series} \end{cases}$

γ (β_1 is correlation angle)

σ $(\delta_o)_{10}$ given in range $\sigma = 0.4$ to 2.0

φ Applicable camber limited by section loading to $D < 0.62$ with 60 deg implied by $0 < C_{l_o} < 2.4$ in Fig. B-5

Base Aerodynamic Variable Range

M_1 very small effect of M_1 on deviation at i_{ref} was predicted up to limiting M_1, where rapid increase in loss occurs

Re above 2.5×10^5 based on chord length and cascade inlet velocity

Ω data correlated for $\Omega \approx 1.0$ only

Turbulence data not available

Design/Analysis Application Examples

A. Modified Base Equation and Incidence

The NACA/NASA rule has been used for $i \neq i_{ref}$ with the equation (Ref. 67)

$$\delta = \delta_{ref} + (i - i_{ref}) \left(\frac{d\delta}{di}\right)_{ref}$$

Values of κ_1 have been used in Figs. B-3 and B-7 to replace β_1 (Ref. 24)

Application of the NACA/NASA rule to design has frequently included a capability to add an arbitrary angle correction. Examples are in Refs. 23, 24 and 48.

B. Extended Blade Section and Cascade Geometry Limits

Airfoil Section Profiles and Camber Line Shapes

The NACA/NASA rule has been applied to exponential, polynomial and arbitrary camber line shapes with polynomial thickness distribution (Refs. 24, 45, 46, 47)

Cascade Geometry Limits

$\frac{a}{c}$ - equation is given for deviation with $\frac{a}{c}$ as a variable in Ref. 24

σ - Ref. 68 suggests caution in application when σ is low and $\beta_1 > 60$ deg

Blade-To-Blade Surface Radius Change

Equivalent circulation turning angle (see Appendix E) is used in NACA/NASA deviation option in Ref. 48.

Ref. 21 suggests a solidity and thickness/chord ratio correction for average blade-to-blade stream surface slope in meridional projection.

C. Extended Aerodynamic Variable Range

M_1 - correction suggested for M_1 above critical value in Refs. 21, 23.

β_1 - Ref. 68 suggests caution in application when $\beta_1 > 60$ deg

Ω - see radius change above

i - Ref. 67 suggests procedure for determining incidence correction

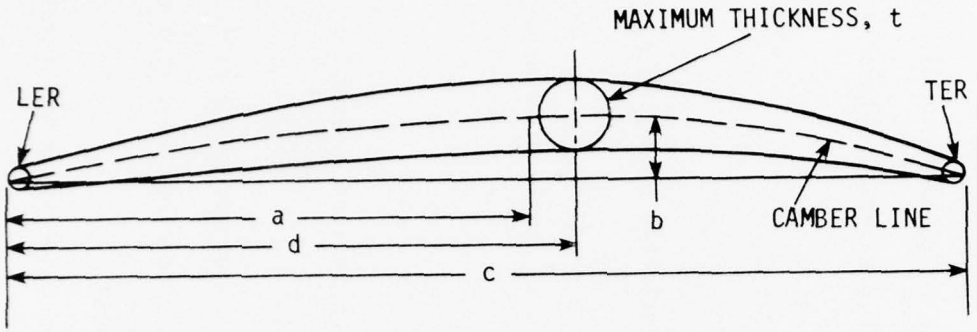

a = LOCATION OF MAXIMUM CAMBER
b = COORDINATE OF MAXIMUM CAMBER
c = CHORD LENGTH
d = LOCATION OF MAXIMUM THICKNESS
LER = LEADING EDGE RADIUS
TER = TRAILING EDGE RADIUS

Figure B-1. NACA/NASA Blade Section Profile Terminology.

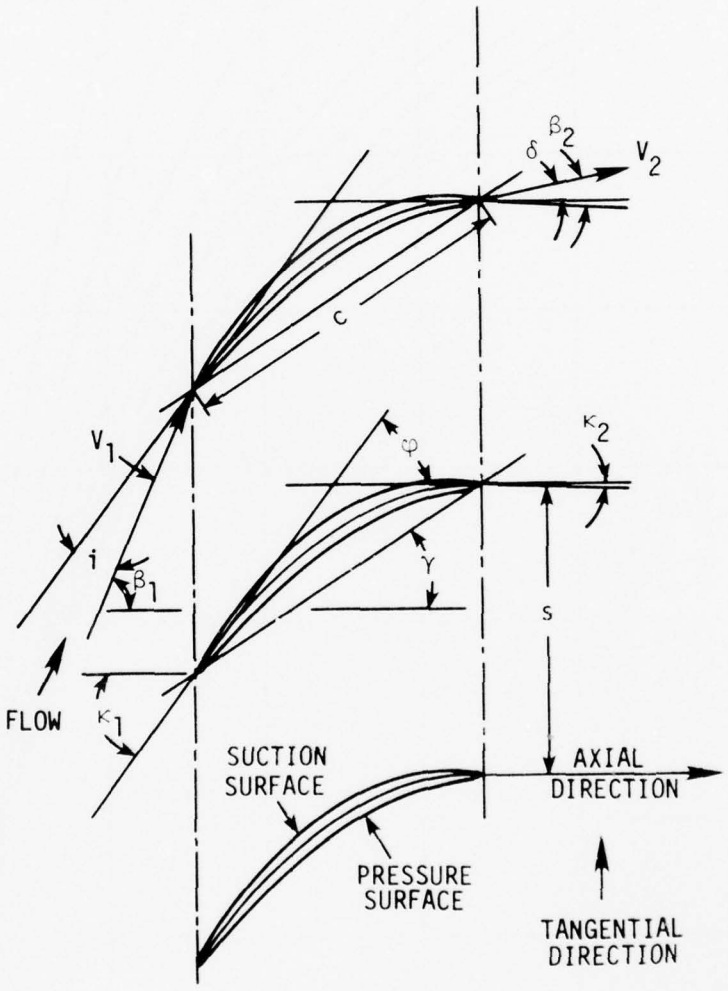

$$i = \beta_1 - \kappa_1 \qquad \Delta\beta = \beta_1 - \beta_2$$

$$\delta = \beta_2 - \kappa_2 \qquad \Delta\beta = \varphi + i - \delta$$

$$\varphi = \kappa_1 - \kappa_2$$

Figure B-2. NACA/NASA Cascade Terminology.

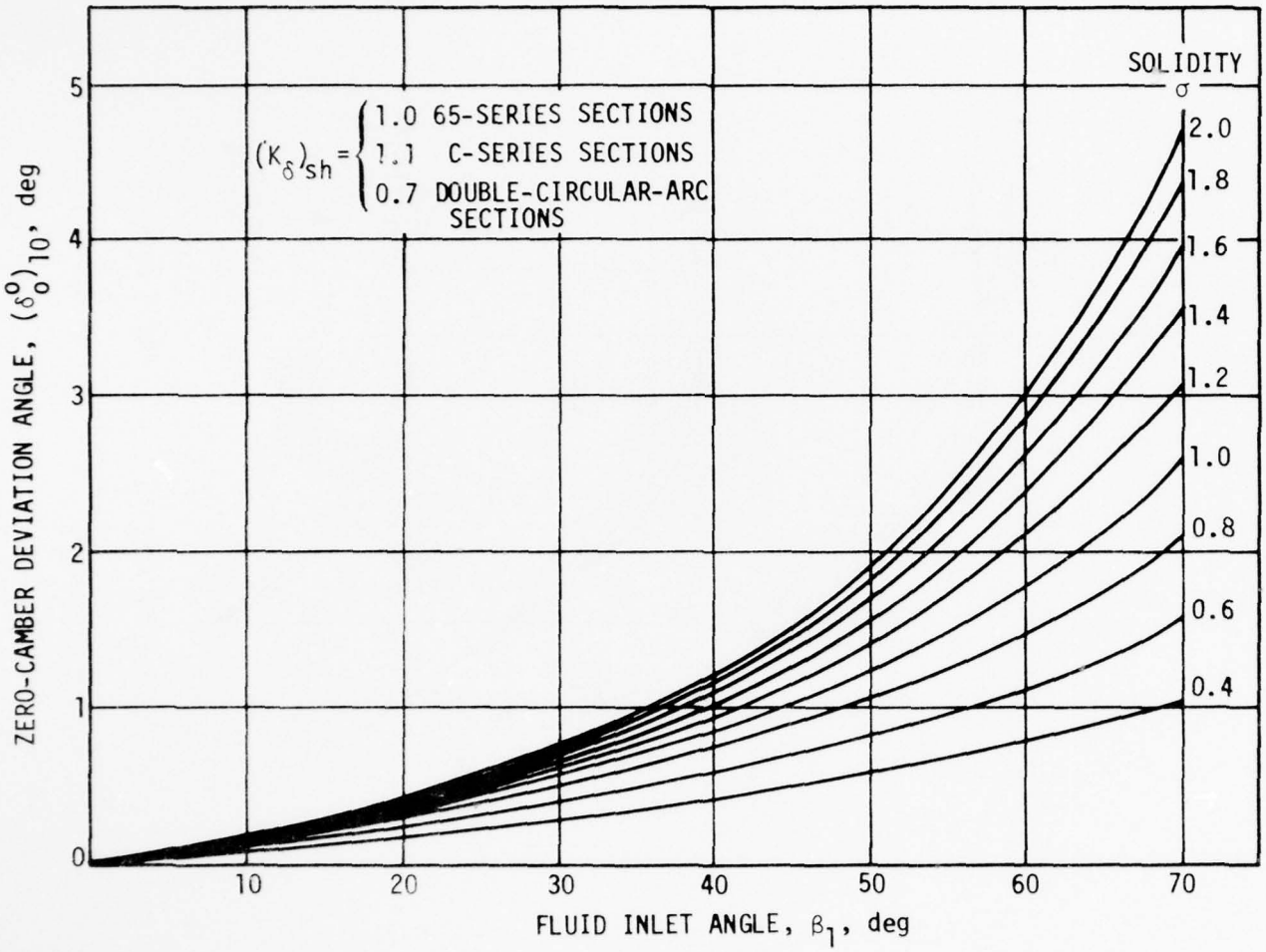

Figure B-3. Zero-Camber Deviation Angle at Reference Minimum-Loss Incidence Angle Deduced from Low-Speed-Cascade Data for 10-Percent-Thick NACA 65-Series Blades.

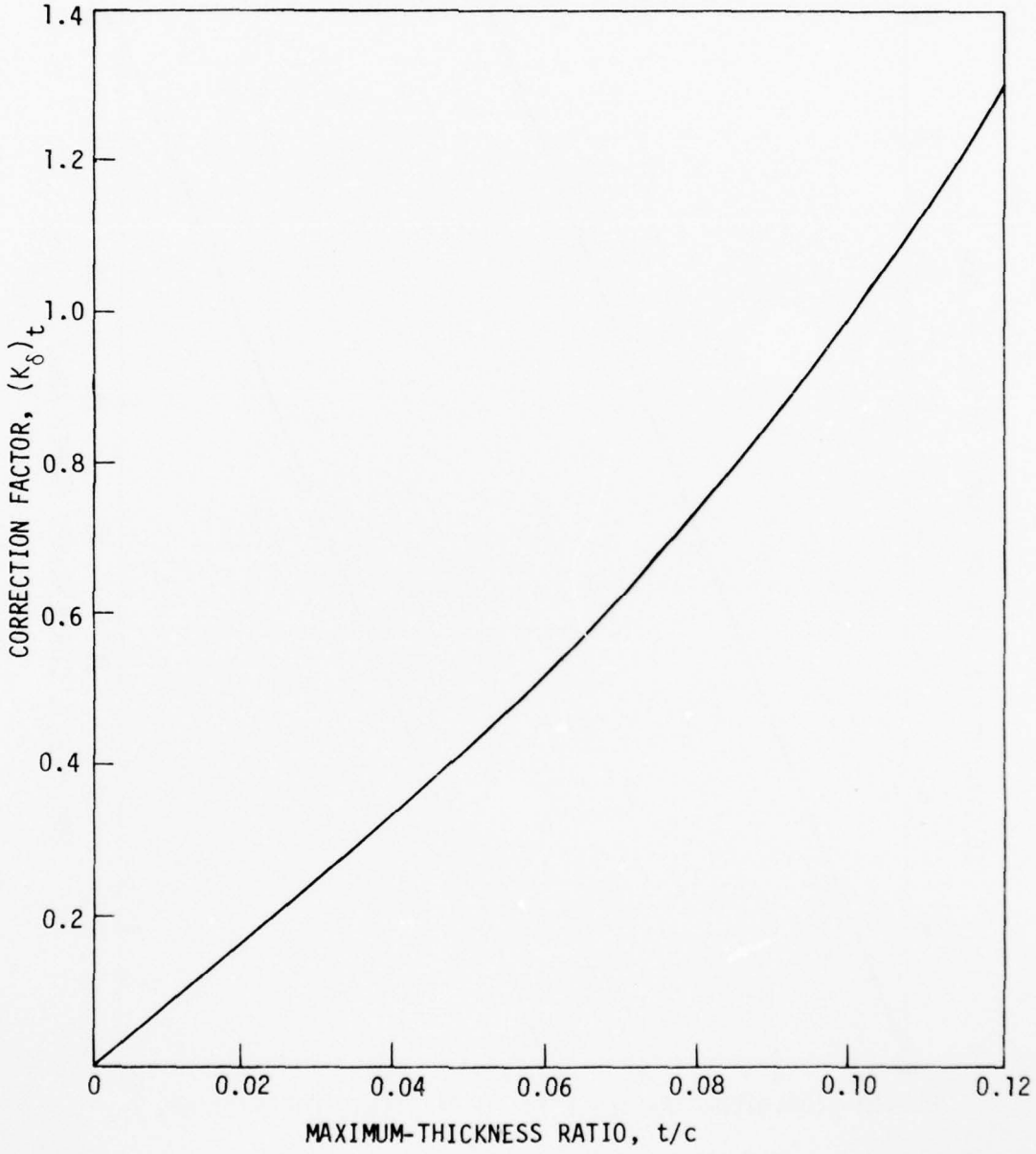

Figure B-4. Maximum-Thickness Correction for Zero-Camber Reference Minimum-Loss Deviation Angle.

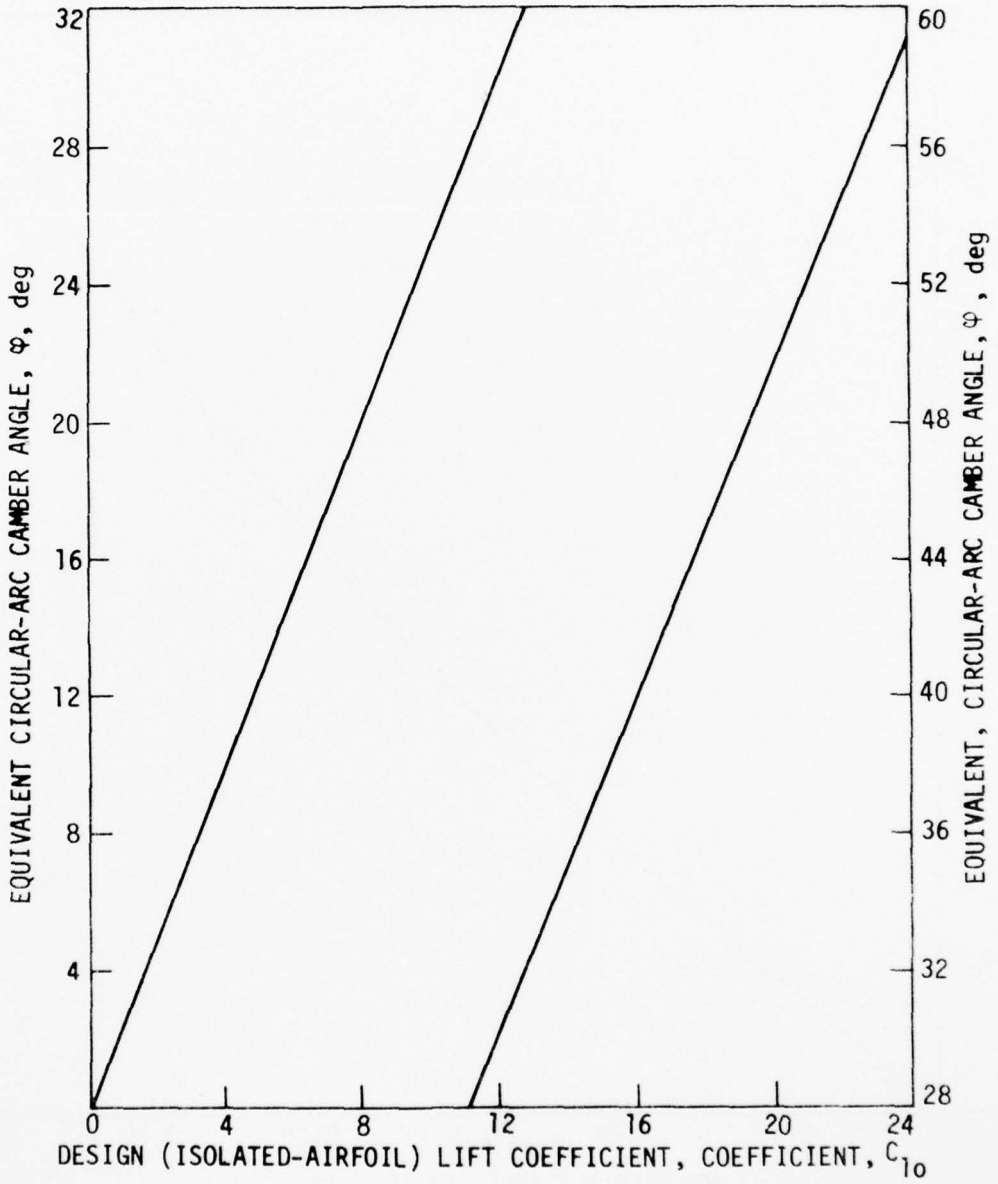

Figure B-5. Equivalent Camber Angles for NACA A_{10} Camber Line as Equivalent Circular Arc (see Ref. 79 for Camber Line Construction with $C_{l_o} \neq 10$).

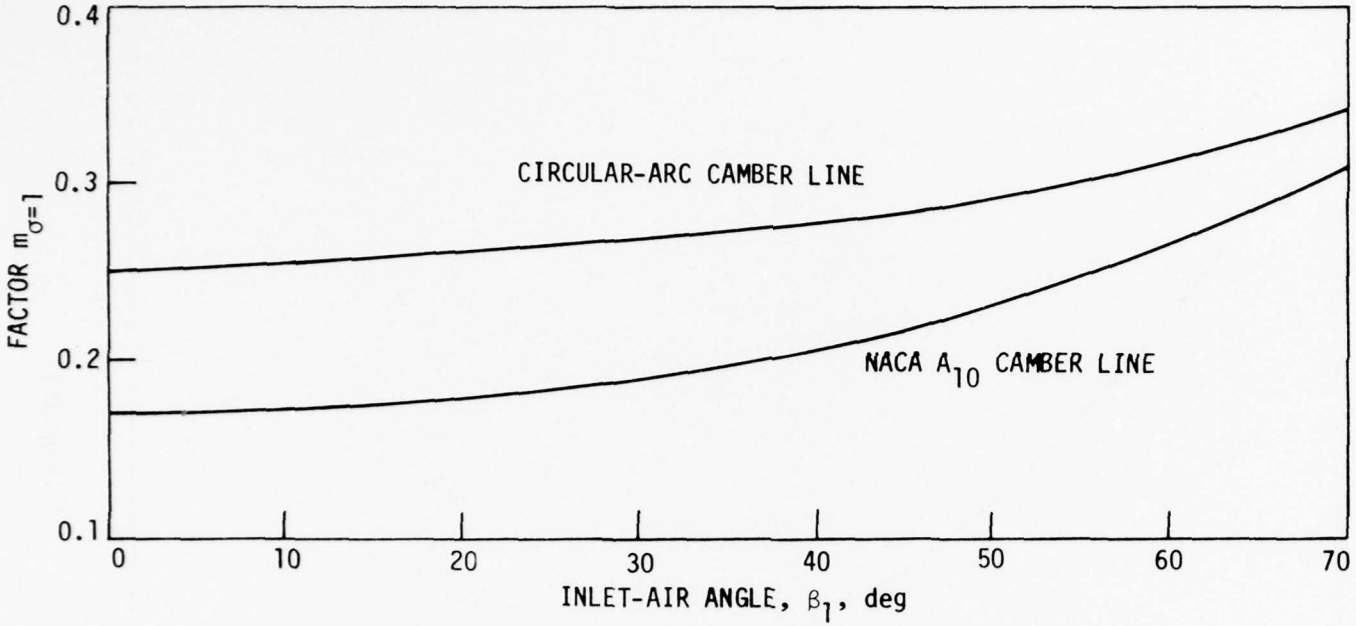

Figure B-6. Factor $m_{\sigma=1}$ in Deviation-Angle Rule.

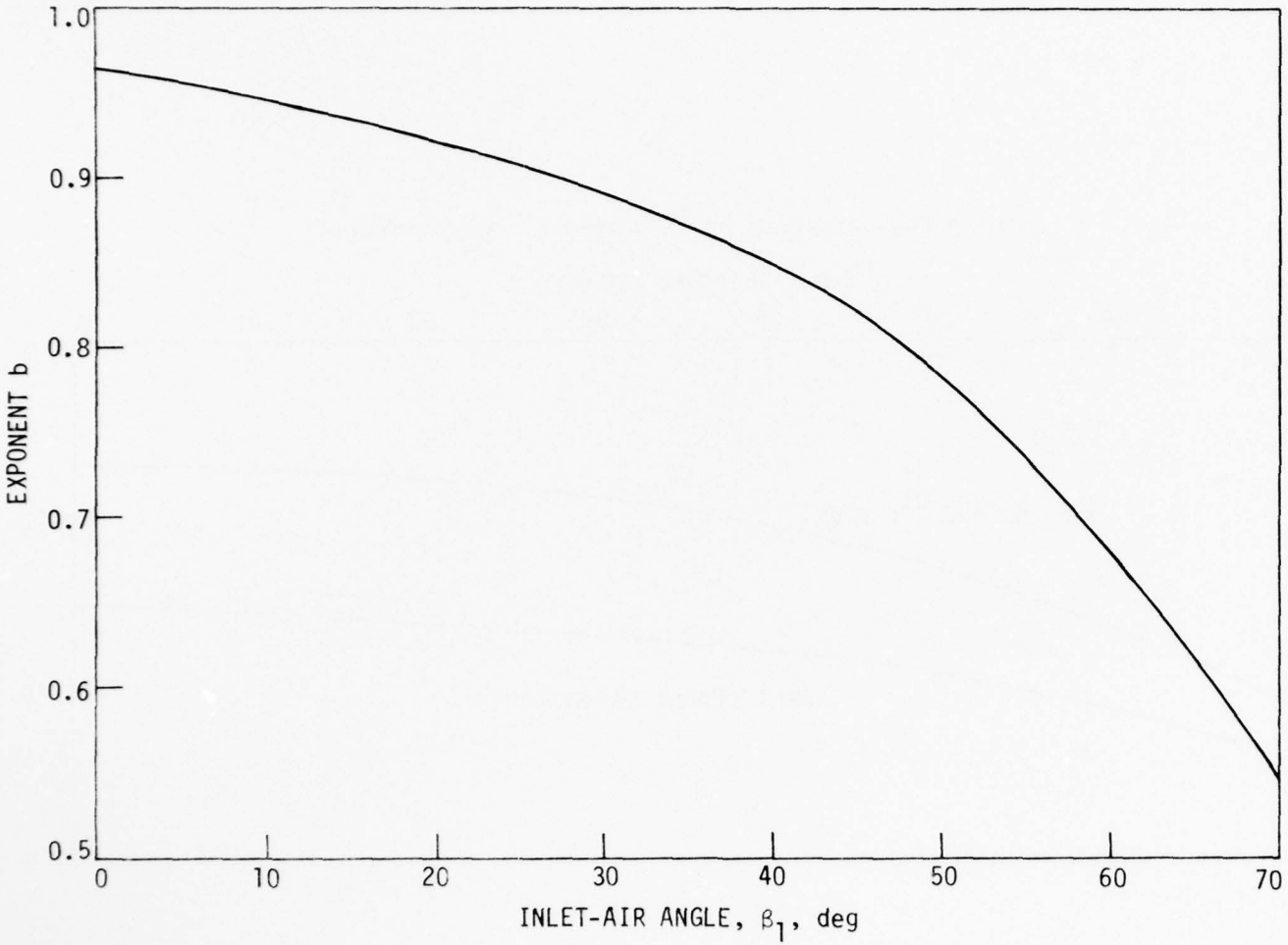

Fig. B-7. Value of Solidity Exponent b in Deviation-Angle Rule Deduced from Data for 65-Series Sections on NACA A_{10} Camber Line

APPENDIX C

USSR FLUID TURNING ANGLE CORRELATION[1]

Base Equation

$$\Delta\alpha_o = \left[\frac{(\Delta\alpha_o)_{\bar{x}_c}}{(\Delta\alpha_o)_{\bar{x}_c = 0.4}}\right]\left[\frac{(\Delta\alpha_o)_{\bar{c}}}{(\Delta\alpha_o)_{\bar{c} = 10\%}}\right]\left[\frac{K\varepsilon}{1000} + B\right]$$

$$K = (5 - 2\,t/b)\sqrt{\nu^2 - 1000\,\frac{t}{b}} + 100\,(5.5 - 2.6\,t/b)$$

$$B = 8\left(\frac{t}{b}\right)^2 - 17\,\frac{t}{b} + 16$$

$$\frac{(\Delta\alpha_o)_{\bar{x}_c}}{(\Delta\alpha_o)_{\bar{x}_c = 0.4}} = 1 - 0.28\,(\bar{x}_c - 0.40) \text{ for } \bar{x}_c = 0.3 \text{ to } 1.0$$

and

$$\frac{(\Delta\alpha_o)_{\bar{c}}}{(\Delta\alpha_o)_{\bar{c} = 10\%}} = 1 - 0.016\,(10 - \bar{c}) \text{ for } \bar{c} = 1.25 \text{ to } 12.5\%$$

At Base Incidence

$$i_o = \alpha_1' - \sin^{-1}\frac{F_\Gamma}{t}$$

---

[1] Symbols and notation in Appendix C correspond to original publication. See also Figures C-1 and C-2.

$\Delta\alpha_o$ fluid turning angle for cascade operation at base incidence i_o and low M_1

ν blade section stagger angle, angle between chord line and tangential direction, degrees

ε blade section camber angle, angle between lines tangent to section camber line at leading and trailing edges, degrees

t blade spacing, tangential distance between equivalent points on adjacent blade section

b chord length, length of straight line connecting points where camber line intersects leading and trailing edges

i angle of incidence, angle between cascade inlet average flow angle and line tangent to blade section camber line at leading edge, degrees

i_o optimum incidence angle, degrees

α_1' blade section camber line angle at leading edge, measured from tangential direction, degrees

α_2' blade section camber line angle at trailing edge, measured from tangential direction, degrees

α_1 average fluid angle at cascade inlet, measured from tangential direction, degrees

α_2 average fluid angle at cascade exit, measured from axial direction, degrees

δ deviation angle, angle between cascade exit average fluid angle and line tangent to blade section camber line at trailing edge, degrees

V_1 fluid velocity at cascade inlet

V_2 fluid velocity at cascade exit

F_Γ minimum flow passage width in blade-to-blade channel (throat) (Ref. 85)

Base Airfoil Section Profile

A-40 symmetric profile (Ref. 86)

(see x_c/ℓ below)

Base Camber Line Shapes

$\Pi 45$ parabolic used for camber angle $\leq$ 55 deg. (Ref. 85)

K50 circular arc for all camber angles $\geq$ 55 deg (Ref. 85)

Base Cascade Geometry Limits

$\frac{x_f}{b}$

- 0.45 parabolic camber line
- 0.50 circular-arc camber line

$\frac{x_c}{\ell}$

- 0.30 A-30
- 0.40 A-40
- 0.50 A-50 (Ref. 85 gives profile construction)
- 0.65 A-65
- 1.00 A-100

$\frac{c}{\ell}$ 0.0125 to 0.125

LER 0.055 c

TER 0.05 c

ν	20 to 110 deg	range of validity suggested in Ref. 86
$\frac{b}{t}$	0.7 to 2.5	
ϵ	5 to 85 deg	

Base Aerodynamic Variable Range[1]

M_1 0.30 to 0.92

Generalized curves are given for predicting change in $\Delta\alpha$ with M_1 in Ref. 86

Re 2×10^5 to 8×10^5 based on chord length and inlet velocity

Ω 1.0 to 1.15

Turbulence not reported

Design/Analysis Application Examples

Not available

---

[1]Values given are ranges reported in Refs. 84-86.

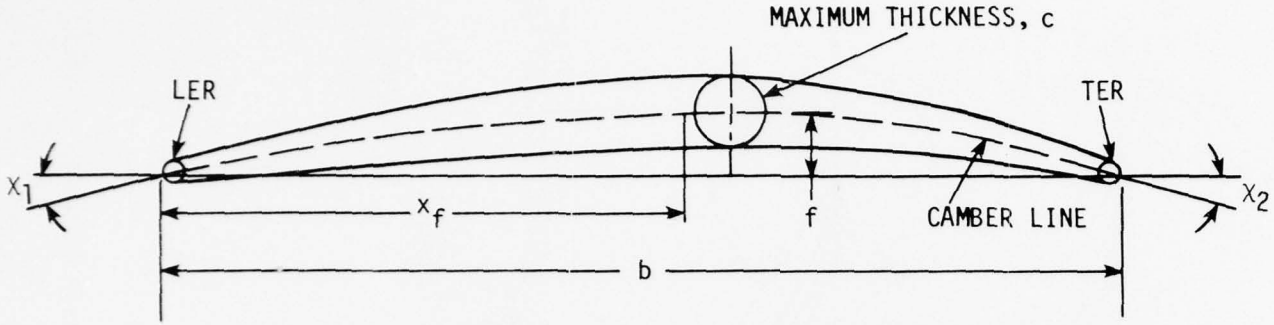

x_f = LOCATION OF MAXIMUM CAMBER
f = COORDINATE OF MAXIMUM CAMBER
b = CHORD LENGTH
x_c = LOCATION OF MAXIMUM THICKNESS
LER = LEADING EDGE RADIUS
TER = TRAILING EDGE RADIUS
χ_1 = ANGLE BETWEEN LINE TANGENT TO BLADE SECTION CAMBER LINE AT LEADING EDGE AND *CHORD LINE, DEGREES*
χ_2 = ANGLE BETWEEN LINE TANGENT TO BLADE SECTION CAMBER LINE AT TRAILING EDGE AND CHORD LINE, DEGREES
l = LENGTH OF CAMBER LINE
$\bar{c} \equiv \frac{c}{l}$ = MAXIMUM RELATIVE THICKNESS

Figure C-1. USSR Blade Section Profile Terminology (Ref. 85).

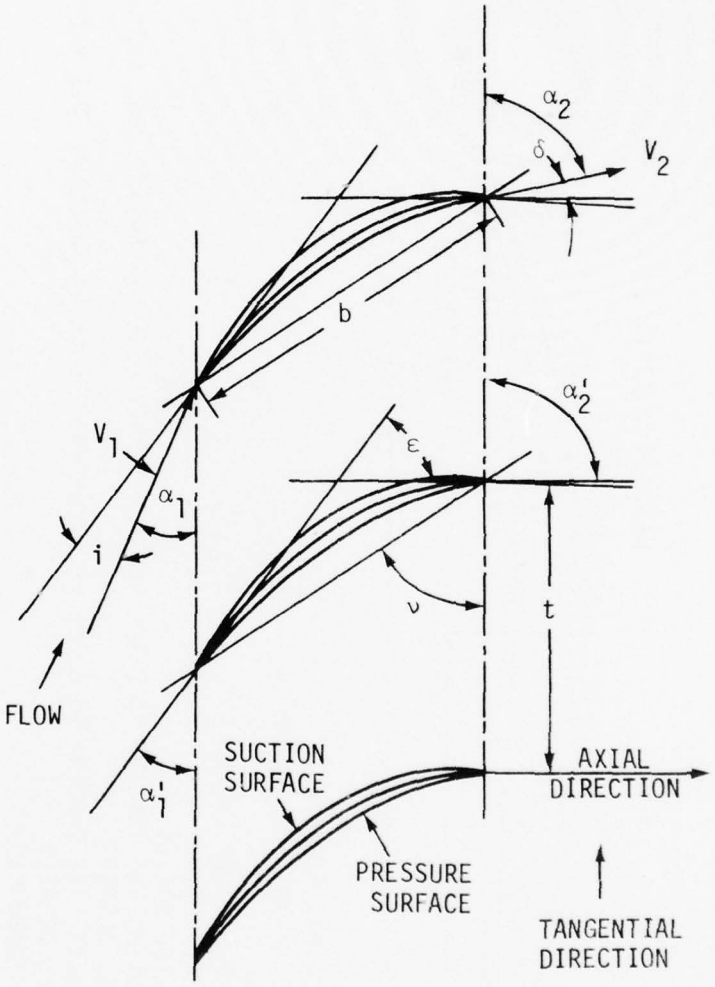

$$i = \alpha'_1 - \alpha_1 \qquad \varepsilon = \alpha'_2 - \alpha'_1$$

$$\delta = \alpha'_2 - \alpha_2 \qquad \Delta\alpha = \varepsilon + i - \delta$$

$$\Delta\alpha = \alpha_2 - \alpha_1$$

Figure C-2. USSR Cascade Terminology (Ref. 85).

AD-A057 804 IOWA STATE UNIV AMES ENGINEERING RESEARCH INST F/G 13/7
DEVIATION ANGLE / TURNING ANGLE PREDICTION FOR ADVANCED AXIAL-F--ETC(U)
DEC 77 G K SEROVY F33615-76-C-2090

UNCLASSIFIED ISU-ERI-AMES-78196 AFAPL-TR-77-81 NL

2 OF 2
AD
A057804

END
DATE
FILMED
10-78
DDC

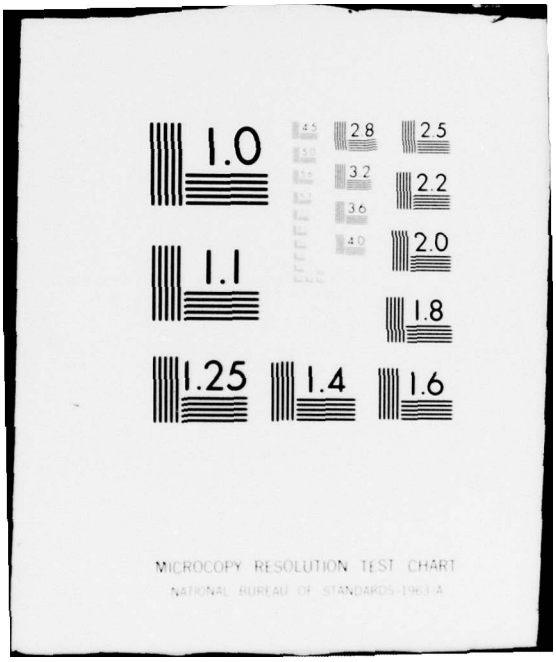
1.0
1.1
1.25
1.4
1.6
1.8
2.0
2.2
2.5
2.8
3.2
3.6
4.0
4.5
5.0
MICROCOPY RESOLUTION TEST CHART
NATIONAL BUREAU OF STANDARDS-1963-A

APPENDIX D

COMPRESSOR BLADE SECTION PROFILES AND CAMBER LINE SHAPES

Table D-1 is a listing of some blade section profile geometries which have been adequately described and have been used in linear cascade experiments or in compressor blade row design. References are given which contain information on or instructions for layout or construction of each profile. In those cases where reasonably general correlation equations exist for aerodynamic performance, reference documents are also listed.

TABLE D-1. COMPRESSOR BLADE SECTION PROFILE GEOMETRIES.

Camber Line	a/c	Typical Thickness Distribution	d/c	t/c	Construction References	Performance Correlation References
NACA a = 1.0	0.50	NACA 65-010 blower blade	0.40	variable from base 0.10	78	78,67,68,114
NACA combination	variable	NACA 65-010 blower blade	0.40	variable from base 0.10	91,78	91,96
Circular arc	0.50	NACA 65-010 blower blade	0.40	variable from base 0.10	69,78	69
		A - series	variable from base 0.40	variable from base 0.10	85	86
		C - series	0.30-0.33	variable from base 0.10	71,82	75
		Double circular arc	0.50	variable	69	
Parabolic						
NGTE	variable	C - series	0.30-0.33	variable from base 0.10	71,82	75
USSR	variable	A - series	variable from base 0.40	variable from base 0.10	85	86
Multiple circular arc						
Type A	variable	circular arc segments	variable	variable	17	--
Type B	variable	circular arc segments	variable	variable	106	--
Type C	variable	parabolic (quadratic equations)	variable	variable	66	--
Type D	variable	third-order polynomial	variable	variable	116,45,47	--
Exponential	variable	third-order polynomial	variable	variable	116,45,47	--
Polynomial	variable	third-order polynomial	variable	variable	116,45,47	--
$d\epsilon/dl$ = constant	variable	surface $d\epsilon/d(\text{surface})$ = constant	variable	variable	48	--
ARL arbitrary	variable	third-order polynomial	variable	variable	46,47	--
NACA arbitrary	variable	variable	arbitrary	arbitrary	117,118	--

APPENDIX E

DERIVATION OF EQUIVALENT CIRCULATION FLUID TURNING ANGLE

The equivalent circulation fluid turning angle concept was developed to rationalize the use of correlations and parameters based on two-dimensional linear cascade experiments for the design and analysis of axial-flow compressor blade rows. In this context it accounts for the influence on effective cascade diffusion loading of changes in stream surface radius and meridional or axial velocity across the blade row.

An example velocity diagram for a rotating compressor cascade with $r_2 \neq r_1$ is shown in Figure E-1. The relative fluid turning angle indicated is

$$\Delta\beta = \beta_1 - \beta_2$$

and the circulation for the row is

$$\Gamma_{row} = r_2 V_{\theta,2} - r_1 V_{\theta,1}$$

If the flow through the rotor occured with no change in radius but with the same total circulation, the equivalent exit tangential velocity would be

$$V_{\theta,2e} = \frac{r_2}{r_1} V_{\theta,2}$$

and

$$W_{\theta,2e} = U_{2e} - V_{\theta,2e} = U_1 - \frac{r_2}{r_1} V_{\theta,2}$$

The equivalent circulation velocity diagram is based on these exit tangential velocity components and

$$V_{m,2e} = V_{m,1}$$

The equivalent relative fluid angle at the rotor exit is

$$\beta_{2e} = \tan^{-1} \frac{U_1 - \frac{r_2}{r_1} V_{\theta,2}}{V_{m,1}}$$

and

$$\Delta\beta_e = \beta_1 - \beta_{2e}$$

$$= \beta_1 - \tan^{-1} \left\{ \frac{r_2 V_{m,2}}{r_1 V_{m,1}} \tan\beta_2 + \frac{U_1}{V_{m,1}} \left[1 - \left(\frac{r_2}{r_1} \right)^2 \right] \right\} \qquad \text{(E-1)}$$

For a stationary blade row

$$\Delta\beta_e = \beta_1 - \tan^{-1} \left[\frac{r_2 V_{m,2}}{r_1 V_{m,1}} \tan\beta_2 \right] \qquad \text{(E-2)}$$

In both the rotor and stator cases the equations for $\Delta\beta_e$ show that both $V_{m,2} < V_{m,1}$ and $r_2 < r_1$ cause an increased equivalent turning angle.

The equivalent circulation approach was suggested in 1957 by Lieblein (Ref. 61) as a means for extending the application of two-dimensional linear cascade diffusion loading parameters to compressor flow conditions. It also is similar to a method for correction of linear cascade turning angles for axial velocity changes used by Erwin and Emery (Ref. 87). The idea was further developed by Klapproth (Ref. 114) for diffusion parameters and was subsequently modified by Seyler and Smith (Ref. 17) and Wright (Ref. 69) to determine equivalent turning angles for deviation angle prediction. Equivalent circulation turning angles have been used for selection of compressor cascade geometries based on cascade plane projection (Ref. 17) and on the conical stream surface approximation (Ref. 48).

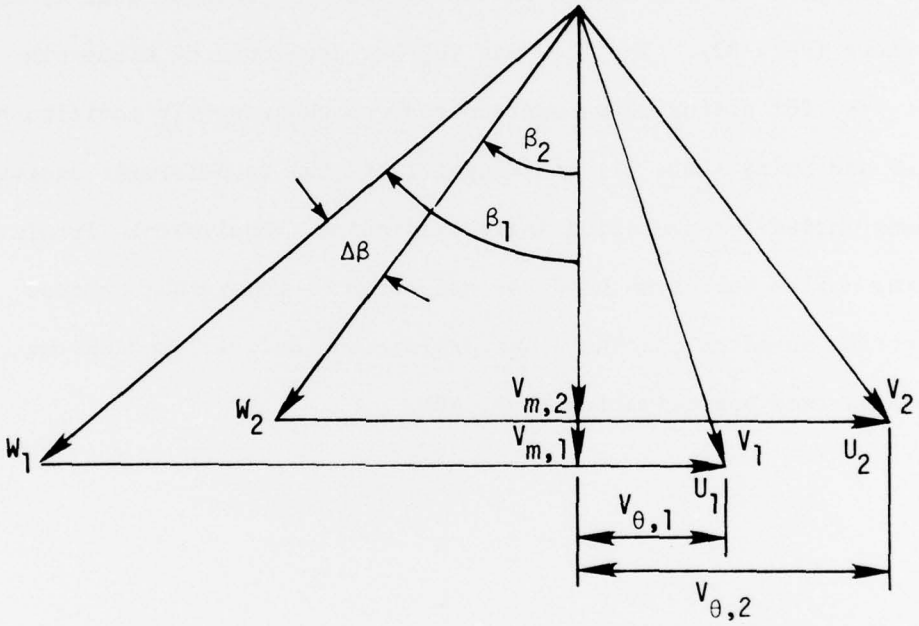

Figure E-1. Rotating Cascade Velocity Diagram Components.

SYMBOLS AND NOTATION

The symbols and notation defined below are recommended for correlation of deviation/fluid turning angle data as described in the body of the report. Separate lists are given for existing correlation systems in the Appendices.

AVR	axial-velocity ratio across blade row, $V_{x,2}/V_{x,1}$
a	location of maximum camber point (see Fig. 5)
a_o	acoustic velocity at local total temperature
b	maximum camber (see Fig. 5)
b	exponent (see Eq. (15) and Appendix B)
c	chord length (see Figs. 5 and 6)
D	cascade diffusion parameter (see Eq. 11)
D_{eq}	cascade equivalent diffusion parameter (see Eq. 12)
d	location of maximum blade section profile thickness (Fig. 5)
e	location of camber line inflection point (see Fig. 8)
H	boundary-layer form factor (see Eq. 7)
i_c	incidence angle, angle between cascade entrance relative flow direction and line tangent to camber line at leading edge (see Fig. 6)
i_{ss}	suction surface incidence angle, angle between cascade entrance flow direction and line tangent to suction surface where leading edge shape fairs into thickness distribution
l	arc length of camber line (see Figs. 5 and 8)
m_c	parameter in NGTE deviation angle correlation (see App. B)
m_{cm}	modified parameter in deviation angle correlation equation (see Eq. 20)

M_R Mach number corresponding to rotor blade velocity (see Eq. 5)

N number of blades in row

P local total pressure

$\bar{P}$ average total pressure

p local static pressure

$\bar{p}$ average static pressure

r radial coordinate (see Fig. 3a)

s blade spacing, distance in tangential or circumferential direction between corresponding points on adjacent blades (see Fig. 6)

t maximum thickness of blade section profile (see Fig. 5)

U blade velocity

V fluid velocity

W fluid velocity measured relative to rotating blade row

X coordinate parallel to chord line (see Fig. 5)

x axial coordinate direction (see Figs. 3)

Y coordinate perpendicular to chord line (see Fig. 5)

y tangential coordinate direction in linear cascade arrangement (see Fig. 7)

z spanwise coordinate in linear cascade arrangement (see Fig. 3b)

Greek

β fluid angle of relative flow measured from axial direction (see Fig. 6)

Γ blade section circulation

γ	blade-chord angle or stagger angle, angle between blade section chord line and axial direction
γ	specific-heat ratio
δ	deviation angle, angle between cascade exit relative flow direction and line tangent to camber line at trailing edge (see Fig.6)
δ^*	boundary layer displacement thickness
θ	tangential or circumferential coordinate in compressor (see Fig.6)
θ^*	boundary layer momentum thickness
κ	camber line angle, angle between line tangent to camber line and axial direction
ρ	fluid density
σ	cascade solidity (see Eq. 1 and 13)
φ	blade section camber angle (see Fig. 6 and Sec.IV)
Ω	axial velocity-density ratio (see Eq. 2)
ω	angular velocity of rotor
$\bar{\omega}$	total-pressure less coefficient (see Eq. 3 and 4)

Subscripts

c	component on cylindrical cascade projection surface
m	meridional component
o	zero-camber in NACA/NASA correlation; optimum in USSR correlation (see App. C)
p	profile
ps	pressure surface
r	radial component
ref	reference minimum-loss

rel	measured relative to rotating blade row
s	inflection point (see Fig. 8, Section 10.2)
ss	suction surface
x	axial component
θ	circumferential component
1	cascade entrance
2	cascade exit

REFERENCES

1. Lorenz, H. "Theorie und Berechnung der Vollturbinen und Kreiselpumpen." VDI Zeitschrift. 49:1670-1675. 1905.

2. Traupel, Walter. "Neue allgemeine Theorie der mehrstufigen axialen Turbomaschinen." Dissertation ETH. Zürich. 1942.

3. Wu, Chung-Hua, and Wolfenstein, Lincoln. "Application of Radial-Equilibrium Condition to Axial-Flow Compressor and Turbine Design." NACA Report 955. 1950.

4. Wu, Chung-Hua. "A General Theory of Three-Dimensional Flow in Subsonic and Supersonic Turbomachines of Axial-, Radial-, and Mixed-Flow Types." NACA TN 2604. 1952.

5. Hatch, James E., Giamati, Charles C., and Jackson, Robert J. "Application of Radial-Equilibrium Condition to Axial-Flow Turbomachine Design Including Consideration of Change of Entropy with Radius Downstream of Blade Row." NACA RM E54A20. 1954.

6. Giamati, Charles C., Jr., and Finger, Harold B. "Design Velocity Distribution in Meridional Plane." In: "Aerodynamic Design of Axial-Flow Compressors." Chapter VII, NASA SP-36. 1965.

7. Smith, L. H., Jr. "The Radial-Equilibrium Equation of Turbomachinery." J. Eng. Power. Trans. ASME, Series A. 88:1-12. 1966.

8. Novak, R. A. "Streamline Curvature Computing Procedures for Fluid-Flow Problems." J. Eng. Power. Trans. ASME, Series A. 89:478-490. 1967.

9. Marsh, H. "The Through-Flow Analysis of Axial Flow Compressors." In: "Advanced Compressors." AGARD-LS-39-70. 1970. Paper 2.

10. Horlock, J. H. "On Entropy Production in Adiabatic Flow in Turbomachines." J. Basic Eng. Trans. ASME, Series D. 93:587-593. 1971.

11. Horlock, J. H., and Marsh, H. "Flow Models for Turbomachines." J. Mech. Engr. Sci. 13:358-368. 1971.

12. Wennerstrom, Arthur J. "On the Treatment of Body Forces in the Radial Equilibrium Equation of Turbomachinery." In: Traupel-Festschrift. Juris-Verlag. 1974.

13. Frost, D. H. "A Streamline Curvature Through Flow Computer Program for Analyzing the Flow through Axial-Flow Turbomachines." ARC Rep. and Memo. 3687. 1970.

14. Stuart, A. R., and Hetherington, R. "The Solution of Three-Variable Duct-Flow Equations." In: "Fluid Mechanics, Acoustics, and Design of Turbomachinery." NASA SP-304, Part I, pp. 135-153. 1974.

15. Novak, R. A., and Hearsey, R. M. A Nearly Three-Dimensional Interblade Computing System for Turbomachinery. J. Fluids Eng., Trans. ASME, Series I. 99:154-166. 1977.

16. Doyle, V. L., and Koch, C. C. "Evaluation of Range and Distortion Tolerance for High Mach Number Transonic Fan Stages. Design Report." NASA CR-72720. 1970.

17. Seyler, D. R., and Smith, L. H., Jr. "Single Stage Experimental Evaluation of High Mach Number Compressor Rotor Blading. Part I - Design of Rotor Blading." NASA CR-54581. 1967.

18. Monsarrat, N. T., Keenan, M. J. and Tramm, P. C. "Single-Stage Evaluation of Highly-Loaded High-Mach-Number Compressor Stages." Design Report. NASA CR-72562. 1969.

19. Davis, W. R. "A Computer Program for the Analysis and Design of Turbomachinery-Revision." Ottawa. Carleton University. Division of Aerothermodynamics. Report ME/A71-5. 1971.

20. Davis, W. R. "A Computer Program for the Analysis and Design of the Flow in Turbomachinery, Part B-Loss and Deviation Correlations." Ottawa. Carleton University. Division of Aerothermodynamics. Report ME/A70-1. 1970.

21. Davis, W. R. and Millar, D. A. J. "Axial Flow Compressor Analysis Using a Streamline Curvature Method." Ottawa. Carleton University. Division of Aerothermodynamics. Report ME/A76-3. 1976.

22. Ball, Calvin L., Janetzke, David C. and Reid, Lonnie. "Performance of 1380-Foot-per-Second-Tip-Speed Axial-Flow Compressor Rotor with Blade Tip Solidity of 1.5." NASA TM X-2379. 1972.

23. Novak, Richard A. "Flow Field and Performance Map Computation for Axial-Flow Compressors and Turbines." In: "Modern Prediction Methods for Turbomachine Performance." AGARD-LS-83. 1976.

24. Hearsey, Richard M. "A Revised Computer Program for Compressor Design. Volume I: Theory, Descriptions and User's Instructions." U.S. Air Force Systems Command, ARL TR 75-0001, Volume I. 1975.

25. Hearsey, Richard M. "A Revised Computer Program for Axial Compressor Design. Volume II: Program Listing and Program Use Example." Aerospace Research Laboratories. ARL TR 75-0001, Volume II. 1975.

26. Erdos, John, Alzner, Edgar, Kalben, Paul, McNally, William, and Slutsky, Simon. "Time-Dependent Transonic Flow Solutions for Axial Turbomachinery." In: "Aerodynamic Analyses Requiring Advanced Computers." NASA SP-347, Part I, pp. 587-621. 1975.

27. Schmidt, D. P., and Okiishi, T. H. "Multistage Axial-Flow Turbomachine Wake Production, Transport, and Interaction." Iowa State University, Engineering Research Institute. ISU-ERI-Ames-77130. TCRL-7. 1976.

28. Lockhart, R. C., and Walker, G. J. "The Influence of Viscous Interactions on the Flow Downstream of an Axial Compressor Stage." Proc. of the 2nd International Symposium on Air Breathing Engines. University of Sheffield. Royal Aeronautical Society, London. 1974.

29. Kerrebrock, J. L., and Mikolajczak, A. A. "Intrastator Transport of Rotor Wakes and Its Effect on Compressor Performance." J. Eng. Power. Trans. ASME, Series A. 92:359-368. 1970.

30. Jansen, W. "The Application of End-Wall Boundary Layer Effects in the Performance Analysis of Axial Compressors." ASME Paper 67-WA/GT-11. 1967.

31. Stratford, B. S. "The Use of Boundary Layer Techniques to Calculate the Blockage from the Annulus Boundary Layers in a Compressor." ASME Paper 67-WA/GT-7. 1967.

32. Mellor, G. L., and Wood, G. M. "An Axial-Compressor End-Wall Boundary-Layer Theory." J. Basic Eng. Trans. ASME, Series D. 93:300-318. 1971.

33. Horlock, J. H., and Hoadley, P. "Calculation of the Annulus Wall Boundary Layers in Axial-Flow Turbomachines." ARC CP 1196. 1972.

34. Horlock, J. H., and Perkins, H. J. "Annulus Wall Boundary Layers in Turbomachines." AGARD-AG-185. 1974.

35. Bosman, C. and El-Shaarawi, M. A. I. "Quasi-Three-Dimensional Numerical Solution of Flow in Turbomachines." J. Fluids Eng. Trans. ASME, Series I. 99:132-140. 1977.

36. Föttner, Leonhard. "Ein Verfahren zum Bestimmen der Verlutbehafteten Trannsonischen Schaufelgitterströmung bei vorgegebener Druckverteilung." Forsch. Ing.-Wes. 38(3):69-81. 1972.

37. Wilkinson, D. H. "Calculation of Blade-to-Blade Flow in a Turbomachine by Streamline Curvature." ARC Rep. and Memo. 3704. 1970.

38. Miller, Max J. and Serovy, George K. "Deviation Angle Estimation for Axial-Flow Compressors Using Inviscid Flow Solutions." J. Eng. Power. Trans. ASME, Series A. 97:163-172. 1975.

39. Delaney, Robert A. and Kavanagh, Patrick. "Transonic Flow Analysis in Axial-Flow Turbomachinery Cascades by a Time-Dependent Method of Characteristics." J. Eng. Power. Trans. ASME, Series A. 98:356-364. 1976.

40. Dodge, P. R. "Transonic Two-Dimensional Flow Analysis of Compressor Cascade with Splitter Vanes." U.S. Air Force Systems Command, AFAPL-TR-75-110. 1975.

41. Geller, Wolfgang. "Theoretische Untersuchung des Einflusses der Lage des Grenzschicht umschlagpunktes auf Umlenkung und Verluste der Schaufelgitterströmung." Zeit. Flugwiss. 24:13-16. 1976.

42. Sanger, Nelson, L. "Two-Dimensional Analytical and Experimental Performance Comparison for a Compressor Stator Section with D-Factor of 0.47." NASA TN D-7425. 1973.

43. Gostelow, J. P. "Review of Compressible Flow Theories for Airfoil Cascades." J. Eng. Power. Trans. ASME, Series A. 95:281-292. 1973.

44. Lichtfuss, H. J. and Starken, H. "Supersonic Cascade Flow." In: Progress in Aerospace Science, Vol. 15, pp. 37-149. New York Pergamon Press, Ltd. 1974.

45. Frost, G. R., Hearsey, R. M. and Wennerstrom, A. J. "A Computer Program for the Specification of Axial Compressor Airfoils." Aerospace Research Laboratories. ARL 72-0171. 1972.

46. Frost, G. R., and Wennerstrom, A. J. "The Design of Axial Compressor Airfoils Using Arbitrary Camber Lines." Aerospace Research Laboratories. ARL-73-0107. 1973.

47. Frost, G. R. "Modifications to ARL Computer Programs Used for Design of Axial Compressor Airfoils." Aerospace Research Laboratories. ARL 74-0060. 1974.

48. Crouse, James E. "Computer Program for Definition of Transonic Axial-Flow Compressor Blade Rows." NASA TN D-7345. 1974.

49. Smith, Leroy H., Jr. and Yeh, Hsuan. "Sweep and Dihedral Effects in Axial-Flow Turbomachinery." J. Basic Eng. Trans. ASME, Series D. 85:401-416. 1963.

50. Schimming, P. and Starken, H. "Data Reduction of Two-Dimensional Cascade Measurements." In: "Modern Methods of Testing Rotating Components of Turbomachines (Instrumentation)." AGARD-AG-207. 1975.

51. Starken, H. and Schimming, P. "Auswertverfahren von Zweidimension alen Gitermessungen." DLR-Mitt. 72-03. 1972.

52. Lieblein, Seymour and Roudebush, William H. "Theoretical Loss Relations for Low-Speed Two-Dimensional-Cascade Flow." NACA TN 3662. 1956.

53. Lieblein, Seymour and Roudebush, William H. Low-Speed Wake Characteristics of Two-Dimensional Cascade and Isolated Airfoil Sections. NACA TN 3771. 1956.

54. Scholz, Norbert. Über die Durchführung systematischer Messungen an ebenen Schaufelgittern. Zeit. für Flugwiss. 4:313-333. 1956.

55. Stewart, Warner L. "Analysis of Two-Dimensional Compressible-Flow Loss Characteristics Downstream of Turbomachine Blade Rows in Terms of Basic Boundary-Layer Characteristics." NACA TN 3515. 1955.

56. Amecke, J. "Anwendung der transsonischen Ähnlichkeitsregel auf die Strömung durch ebene Schaufelgitter." VDI-Forchungsheft 540, pp. 16-28. 1970. (Dissertation TU Braunschweig 1969)

57. Dzung, L. S. "Consistent Mean Values for Compressible Media in the Theory of Turbomachines." Brown Boveri Review. 58(10):3-10. 1971.

58. Mikolajczak, A. A., Morris, A. L. and Johnson, B. V. "Comparison of Performance of Supersonic Blading in Cascade and in Compressor Rotors." J. Eng. Power. Trans. ASME, Series A. 93:42-48. 1971.

59. Fleeter, Sanford, Holtman, Robert L., McClure, Robert B. and Sinnet, George T. "Experimental Investigation of a Supersonic Compressor Cascade." Aerospace Research Laboratories., ARL TR 75-0208. 1975.

60. Lieblein, Seymour, Schwenk, Francis C. and Broderick. Robert L. "Diffusion Factor for Estimating Losses and Limiting Blade Loadings in Axial-Flow-Compressor Blade Elements." NACA RM E53D01. 1953.

61. Lieblein, Seymour. "Analysis of Experimental Low-Speed Loss and Stall Characteristics of Two-Dimensional Compressor Blade Cascades." NACA RM E57A28. 1957.

62. Thompkins, William T., Jr. and Oliver, David A. "Three-Dimensional Flow Calculation for a Transonic Compressor Rotor." In: "Through-Flow Calculations in Axial Turbomachinery." AGARD-CP-195. 1976. Paper 6.

63. Dunker, R., Schodl, R., and Weyer, H. B. "Fortschritte in der Turbomaschinen forschung durch ein neues optisches Messverfahren für Strömungsvektoren." Zeit. Flugwiss. 24:17-25. 1976.

64. Dunker, R. J., Strinning, P. E., and Weyer, H. B. "Experimental Study of the Flow Field Within a Transonic Axial Compressor Rotor by Laser Velocimetry and Comparison With Through-Flow Calculations." ASME Paper 77-GT-28. 1977.

65. Ruggeri, Robert S. and Benser, William A. "Performance of a Highly-Loaded Two-Stage Axial-Flow Fan." NASA TM X-3076. 1974.

66. Huffman, G. D. and Tramm, P. C. "Airfoil Design for High Tip Speed Compressors." J. Aircr. 11:682-689. 1974.

67. Lieblein, Seymour. "Experimental Flow in Two-Dimensional Cascades." In: "Aerodynamic Design of Axial Flow Compressors." Chapter VI, NASA SP-36. 1965.

68. Lieblein, Seymour. "Incidence and Deviation-Angle Correlations for Compressor Cascades." J. Basic Eng. Trans. ASME, Series D. 82:575-587. 1960. (Discussions by L. H. Smith, Jr. and G. Sovran relate to β_1, σ limits).

69. Wright, L. C. "Blade Selection for a Modern Axial-Flow Compressor." In: NASA SP-304, Part 2, pp. 603-626. 1974.

70. Constant, H. "Performance of Cascades of Aerofoils." R.A.E. Note No. E.3696. A.R.C. 4155. 1939. (Unpublished)

71. Howell, A. R. "The Present Basis of Axial Flow Compressor Design. Part I. Cascade Theory and Performance." Aeronautical Research Council. Rep. and Memo. No. 2095. 1942.

72. Howell, A. R. "Fluid Dynamics of Axial Compressors." Proc. of the IME. 153:441-452. 1945.

73. Howell, A. R. "Note on the Theory of Arbitrary Aerofoils in Cascade." Philos. Mag., Series 7, 39:913-927. 1948.

74. Carter, A. D. S. and Hughes, Hazel P. "A Theoretical Investigation into the Effect of Profile Shape on the Performance of Aerofoils in Cascade." ARC Rep. and Memo. 2384. 1950.

75. Carter, A. D. S. "The Low Speed Performance of Related Aerofoils in Cascades." ARC CP 29. 1950.

76. Weinig, F. Die Strömung um die Schaufeln von Turbomaschinen. Leipzig. J. A. Barth. 1935.

77. Schlichting, Hermann. "Problems and Results of Investigations on Cascade Flow." J. Aero. Sci. 21:163-178. 1954.

78. Emery, James C., Herrig, L. Joseph, Erwin, John R. and Felix A. Richard. "Systematic Two-Dimensional Cascade Tests of NACA 65-Series Compressor Blades at Low Speeds." NACA Report 1368. 1958.

79. Herrig, L. Joseph, Emery, James C. and Erwin, John R. "Effect of Section Thickness and Trailing-Edge Radius on the Performance of NACA 65-Series Compressor Blades in Cascade at Low Speeds." NACA RM L51 J16. 1951.

80. Felix, A. Richard and Emery, James C. "A Comparison of Typical National Gas Turbine Establishment and NACA Axial-Flow Compressor Blade Sections in Cascade at Low Speed." NACA TN 3937. 1957.

81. Andrews, S. J. "Tests Related to the Effect of Profile Shape and Camber Line on Compressor Cascade Performance." ARC Rep. and Memo. 2743. 1955.

82. Howell, A. R. "A Note on the Compressor Base Aerofoils C.1, C.2, C.3, C.4, C.5, and Aerofoils Made up of Circular Arcs." Power Jets, Ltd. Memo M. 1011. September 1944.

83. Miller, Max J. and Skånberg, Torbjorn. "Reference Incidence Angles in Constant Stagger Cascades." Iowa State University. ISU-ERI-Ames-99985. June 1971.

84. Komarov, A. P. "Investigation of Flat Compressor Grids." FTD-MT-24-69-68. 26 April 1968. Translation of "Lopatochnyye Mashiny i Struynyye Apparaty." Sbornik Statey. Vypusk 2. Moscow. Izdatel'stvo Mashinostroyeniye. 1967. pp. 67-110. AD 682829.

85. Bunomovich. A. I. and Svyatogorov, A. A. "Aerodynamic Characteristics of Foil Compressor Cascades at High Subsonic Speed." FTD-MT-24-69-68. 26 April 1968. Translation of "Lopatochnyye Mashiny i Struynyye Apparaty." Sbornik Statey. Vypusk 2. Moscow. Izdatel' stvo Mashinostroyeniye. 1967. pp. 5-35. AD 682829.

86. Bunimovich, A. I. and Svyatogorov, A. A. "Generalization of Results of Investigation of Foil Compressor Cascades at Subsonic Speed." FTD-MT-24-69-68. 26 April 1968. Translation of "Lopatochnyye Mashiny i Struynyye Apparaty." Sbornik Statey. Vypusk 2. Moscow. Izdatel'stvo Mashinostroyeniye. 1967. pp. 36-66. AD 682829.

87. Erwin, John R. and Emery, James C. "Effect of Tunnel Configuration and Testing Technique on Cascade Performance." NACA Report 1016. 1950.

88. Emery, James C. "Low-Speed Cascade Investigation of Thin Low-Camber NACA 65-Series Blade Sections at High Inlet Angles." NACA RM L57E03. 1957.

89. Savage, Melvyn, Felix, A. Richard and Emery, James C. "High-Speed Cascade Tests of a Blade Section Designed for Typical Hub Conditions of High-Flow Transonic Rotors." NACA RM L55F07. 1955.

90. Emery, James C. "Low-Speed Cascade Investigation of Loaded Leading-Edge Compressor Blades." NACA TN 4178. 1957.

91. Erwin, John R., Savage, Melvyn and Emery, James C. "Two-Dimensional Low-Speed Cascade Investigation of NACA Compressor Blade Sections Having a Systematic Variation in Mean-Line Loading." NACA TN 3817. 1956.

92. Dunavant, James C., Emery, James C., Walch, Howard C. and Westphal, Willard R. "High-Speed Cascade Tests of the NACA 65-($12A_{10}$) 10 and NACA 65-($12A_2I_{8b}$) 10 Compressor Blade Sections." NACA RM L55I08. 1955.

93. Emery, James C. and Dunavant, James C. "Two-Dimensional Cascade Tests of NACA 65-($C_{10}A_{10}$) 10 Blade Sections at Typical Compressor Hub Conditions for Speeds Up to Choking." NACA RM L57H05. 1957.

94. Dunavant, James C. and Emery, James C. "Two-Dimensional Cascade Investigation at Mach Numbers Up to 1.0 of NACA 65-Series Blade Sections at Conditions Typical of Compressor Tips." NACA RM L58A02. 1958.

95. Briggs, William, B. "Effect of Mach Number on the Flow and Application of Compressibility Corrections in a Two-Dimensional Subsonic-Transonic Compressor Cascade Having Varied Porous-Wall Suction at the Blade Tips." NACA TN 2649. 1952.

96. Heilmann, W. "Experimentelle und Grenzschichttheoretische Untersuchungen an Ebenen Verzögerungsgittern bei Kompressibler Strömung, inbesondere bei Änderung des Axialen Strömdichteverhältnisses und der Zustromturbulenz." DLR FB 67-88. 1967.

97. Heilmann, W. "The Influence of Axial Velocity Density Ratio on Compressor Cascade Performance in Compressible Flow." In: "Boundary Layer Effects in Turbomachines." AGARD-AG-164. 1972. Paper I-13.

98. Starken, H. "Untersuchung der Strömung in Ebenen Überschallverzögerungsgitlern." DLR FB 71-99. 1971.

99. Starken, H., Breugelmans, F. A. E. and Schimming, P. "Investigation of the Axial Velocity Density Ratio in a High Turning Cascade." ASME Paper 75-GT-25. 1975.

100. Masek, Z. and Norbury, J. F. "Low-Speed Performance of a Compressor Cascade Designed for Prescribed Velocity Distribution and Tested with Variable Axial Velocity Ratio." In: "Heat and Fluid Flow in Steam and Gas Turbine Plant." IME Conference Publication 3, pp. 224-236. 1973.

101. Ilyas, M. and Norbury, J. F. "Effect of Axial Velocity Variation on the Subsonic Flow Through a Compressor Cascade." In: "Heat and Fluid Flow in Steam and Gas Turbine Plant." IME Conference Publication 3, pp. 276-287. 1973.

102. Ohounu, E. H. and Shaw, R. "Effect of Axial Velocity Variation on Deviation for Compressor Cascades." In: "Heat and Fluid Flow in Steam and Gas Turbine Plant." IME Conference Publication 3, pp. 110-114. 1973.

103. Stark, Udo and Starke, Jörg. "Theoretische und experimentelle Untersuchungen über die quasi-zweldimensionale inkompressible Strömung durch vorgegebene ebene Verdichtergitter." Forsch. Ing. Wes. 40:172-186. 1974.

104. Sandercock, Donald M. Unpublished communications concerned with NASA Lewis Research Center fan and compressor data evaluation, 1975-1977.

105. Sulam, D. H., Keenan, M. J. and Flynn, J. T. "Single-Stage Evaluation of Highly-Loaded High-Mach-Number Compressor Stages. II - Data and Performance Multiple-Circular-Arc Rotor." NASA CR-72694. 1970.

106. Keenan, M. J. and Monsarrat, N. T. "Experimental Evaluation of Transonic Stators." Preliminary Analysis and Design Report. NASA CR-54620. 1967.

107. Keenan, M. J. and Bartok, J. A. "Experimental Evaluation of Transonic Stators." Final Report. NASA CR-72298. 1969.

108. Harley, K. G. and Burdsall, E. A. "High-Loading Low-Speed Fan Study. Part 2: Data and Performance, Unslotted Blades and Vanes." NASA CR-72667. 1969.

109. Lewis, G. W., Jr. and Tysl, E. R. "Overall and Blade-Element Performance of a 1.20-Pressure-Ratio Fan Stage at Design Blade Setting Angle." NASA TM X-3101. 1974.

110. Osborne, W. M. and Steinke, R. J. "Performance of a 1.15 Pressure Ratio Axial-Flow Fan Stage with a Blade Tip Solidity of 0.5." NASA TM X-3052. 1974.

111. Kovich, G. and Steinke, R. J. "Performance of a 1.15 Pressure Ratio Axial-Flow Fan Stage with a Blade Tip Solidity of 0.65." NASA TM X-3341. 1976.

112. Moore, R. D. and Steinke, R. J. "Aerodynamic Performance of a 1.25 Pressure-Ratio Axial-Flow Fan Stage." NASA TM X-3083. 1974.

113. Bahr, Jürgen. "Untersuchungen über den Einfluss der Profiledicke auf die kompressible ebene Strömung durch Verdichtergitter." Forsch. Ing. Wes. 30:14-25. 1964.

114. Lieblein, Seymour. "Loss and Stall Analysis of Compressor Cascades." J. Basic Eng., Trans. ASME, Series D., 81:387-397. 1959. (Discussion by J. F. Klapproth relates to D_{eq} for annular cascades.)

115. Wennerstrom, A. J. and Hearsey, Richard M. "The Design of an Axial Compressor Stage for a Total Pressure Ratio of 3 to 1." U.S. Air Force Systems Command. Aerospace Research Laboratories, ARL 71-0061. 1971.

116. Hearsey, Richard M. and Wennerstrom, Arthur J. "Axial Compressor Airfoils for Supersonic Mach Numbers." Aerospace Research Laboratories, ARL 70-0046. 1970.

117. Stanitz, John D. "Approximate Design Method for High-Solidity Blade Elements in Compressors and Turbines." NACA TN 2408. 1951.

118. Klapproth, John F., Jacklitch, John J., Jr. and Tysl, Edward R. "Design and Performance of a 1400-Foot-per-Second-Tip-Speed Supersonic Compressor Rotor." NACA RM E55A27. 1955.

*U.S.Government Printing Office: 1978 — 757-080/723